

# Stabilization of Higher Order Cut Finite Element Methods on Surfaces\*

Mats G. Larson <sup>†</sup> Sara Zahedi <sup>‡</sup>

## Abstract

We develop and analyze a stabilization term for cut finite element approximations of an elliptic second order partial differential equation on a surface embedded in  $\mathbb{R}^d$ . The new stabilization term combines properly scaled normal derivatives at the surface together with control of the jump in the normal derivatives across faces and provides control of the variation of the finite element solution on the active three dimensional elements that intersect the surface which may be used to show that the condition number of the stiffness matrix is  $O(h^{-2})$ , where  $h$  is the mesh parameter. The stabilization term works for higher order elements and the derivation of its stabilizing properties is simple. We also present numerical studies confirming our theoretical results.

## 1 Introduction

**CutFEM for Surface Partial Differential Equations.** CutFEM (Cut Finite Element Method) provides a new high order finite element method for solution of partial differential equations on surfaces. The main approach is to embed the surface into a three dimensional mesh and to use the restriction of the finite element functions to the surface as trial and test functions. More precisely, let  $\Gamma$  be a smooth closed surface embedded in  $\mathbb{R}^3$  with exterior unit normal  $n$  and consider the Laplace-Beltrami problem: find  $u \in H^1(\Gamma)$  such that

$$a(u, v) = l(v) \quad \forall v \in H^1(\Gamma) \quad (1.1)$$

The forms are defined by

$$a(w, v) = \int_{\Gamma} \nabla_{\Gamma} w \cdot \nabla_{\Gamma} v, \quad l(v) = \int_{\Gamma} f v \quad (1.2)$$

---

\*This research was supported in part by the Swedish Foundation for Strategic Research Grant No. AM13-0029, the Swedish Research Council Grants Nos. 2013-4708 and 2014-4804, and the Swedish Research Programme Essence

<sup>†</sup>Department of Mathematics and Mathematical Statistics, Umeå University, SE-90187 Umeå, Sweden

<sup>‡</sup>Department of Mathematics, KTH Royal Institute of Technology, SE-100 44 Stockholm, Sweden

where  $\nabla_\Gamma$  is surface gradient and  $f \in L^2(\Gamma)$  a given function with average zero. Let now  $\Gamma$  be embedded into a polygonal domain  $\Omega$  equipped with a quasiuniform mesh  $\mathcal{T}_{h,0}$  and let  $\Gamma_h$  be a family of discrete surfaces that converges to  $\Gamma$  in an appropriate manner. Let the active mesh  $\mathcal{T}_h$  consist of all elements that intersect  $\Gamma_h$ . Let  $V_h$  be the space of continuous piecewise polynomial functions on  $\mathcal{T}_h$  with average zero on  $\Gamma_h$ . The basic CutFEM takes the form: find  $u_h \in V_h$  such that

$$a_h(u_h, v) = l_h(v) \quad \forall v \in V_h \quad (1.3)$$

where

$$a_h(w, v) = \int_{\Gamma_h} \nabla_\Gamma w \cdot \nabla_\Gamma v, \quad l_h(v) = \int_{\Gamma_h} f_h v \quad (1.4)$$

and  $f_h$  is a suitable representation of  $f$  on  $\Gamma_h$ . In the context of surface partial differential equations this approach, also called trace finite elements, was first introduced in [21] and has then been developed in different directions including higher order approximations in [24], discontinuous Galerkin methods [5], transport problems [23], embedded membranes [9], coupled bulk-surface problems [7] and [15], minimal surface problems [8], and time dependent problems on evolving surfaces [18], [20], [22], and [25]. We also refer to the overview article [2] and the references therein.

**Previous Work on Preconditioning and Stabilization.** The basic CutFEM method (1.3) manufactures a potentially ill conditioned linear system of equations and stabilization or preconditioning is therefore needed. In [19] it was shown that diagonal preconditioning works for piecewise linear approximation and in [24] it was shown that also quadratic elements can be preconditioned if the full gradient is used instead of the tangential gradient in the bilinear form  $a_h$ , see also [10] where this formulation was proposed.

In [3] a stabilized version of (1.3) was introduced. The method takes the form

$$a_h(u_h, v) + s_h(u_h, v) = l(v) \quad \forall v \in V_h \quad (1.5)$$

where  $s_h$  is a stabilization form which is added in order to ensure stability of the method. More precisely we show that there is a constant such that for all  $v \in V_h$ ,

$$\|v\|_{L^2(\mathcal{T}_h)}^2 \lesssim h(a_h(v, v) + s_h(v, v)) \quad (1.6)$$

Using (1.6) and the properties of  $a_h$  we can show that the condition number  $\kappa$  of the stiffness matrix satisfies the optimal bound

$$\kappa \lesssim h^{-2} \quad (1.7)$$

In [3] only piecewise linear finite elements were considered and the stabilization term was defined by

$$s_h(w, v) = c_F([D_{n_F} w], [D_{n_F} v])_{\mathcal{F}_h} \quad (1.8)$$

where  $[D_{n_F}v]$  is the jump in the normal derivative of  $v$  at the face  $F$ ,  $\mathcal{F}_h$  is the set of internal faces (i.e. faces with two neighbors) in the active mesh  $\mathcal{T}_h$ , and  $c_F > 0$  is a stabilization parameter. Optimal order bounds on the error and condition number were established. Furthermore, for linear elements the so called full gradient stabilization

$$s_h(v, w) = h(\nabla v, \nabla w)_{\mathcal{T}_h} \quad (1.9)$$

was proposed and analyzed in [6] as a simpler alternative, and for higher order elements the normal gradient stabilization

$$s_h(w, v) = h^\alpha (n_h \cdot \nabla w, n_h \cdot \nabla v)_{\mathcal{T}_h} \quad \alpha \in [-1, 1] \quad (1.10)$$

was proposed and analysed independently in [4] and [14]. The restrictions on  $\alpha$  essentially comes from a lower bound which implies that optimal order a priori error estimates holds and an upper bound which implies that the desired stability estimate (1.6) holds. Note that stronger control than (1.6) is sometimes demanded, for instance in cut discontinuous Galerkin methods [5], which may lead to stronger upper restrictions on  $\alpha$ .

**New Contributions.** In this work we consider stabilization of higher order elements using a combination of face stabilization and normal derivative stabilization at the actual surface. More precisely the stabilization term takes the form

$$s_h(v, w) = s_{h,F}(v, w) + s_{h,\Gamma}(v, w) \quad (1.11)$$

with

$$s_{h,F}(v, w) = \sum_{j=1}^p c_{F,j} h^{2(j-1+\gamma)} ([D_{n_F}^j v], [D_{n_F}^j w])_{\mathcal{F}_h} \quad (1.12)$$

$$s_{h,\Gamma}(v, w) = \sum_{j=1}^p c_{\Gamma,j} h^{2(j-1+\gamma)} (D_{n_h}^j v, D_{n_h}^j w)_{\Gamma_h} \quad (1.13)$$

where  $\gamma \in [0, 1]$  is a parameter,  $[D_{n_F}^j v]$  is the jump in the normal derivative of order  $j$  across the face  $F$ , and  $c_{F,j} > 0$ ,  $c_{\Gamma,j} > 0$ , are stabilization constants. This stabilization term with  $\gamma = 1$  has also been used in a high order space-time CutFEM on evolving surfaces [25]. We note that also for this stabilization term there is a certain range of scaling with the mesh parameter  $h$ , and in fact the following stronger version of (1.6) holds

$$\|v\|_{L^2(\mathcal{T}_h)}^2 + h^{2\gamma} \|\nabla v\|_{L^2(\mathcal{T}_h)}^2 \lesssim h(a_h(v, v) + s_h(v, v)) \quad (1.14)$$

where we note that we get stronger control of the gradient for smaller  $\gamma \in [0, 1]$ , which corresponds to stronger stabilization.

Using the combination of the face and surface stabilization terms the proof of (1.6) consists of two steps:

- Using the face terms we can estimate the  $L^2$  norm of a finite element function at an element in terms of the  $L^2$  norm at a neighboring element which share a face and the stabilization term on the shared face. Repeating this procedure we can pass from any element to an element which has a large intersection,  $|T \cap \Gamma_h| \gtrsim h^2$ , with  $\Gamma_h$ .
- Using the stabilization of normal derivatives at the surface we can control a finite element function on elements which have large intersection with  $\Gamma_h$ .

Using shape regularity we can show that one can pass from any element in  $\mathcal{T}_h$  to an element with a large intersection in a uniformly bounded number of steps, see [3] and [12].

**Outline.** In Section 2 we introduce the model problem, in Section 3 we formulate the finite element method, in Section 4 we collect some basic preliminary results, in Section 5 we formulate the properties of the stabilization term, in Section 6 we establish an optimal order condition number estimate, in Section 7 we prove optimal order a priori error estimates, and in Section 8 we present numerical results that support our theoretical findings.

## 2 The Laplace-Beltrami Problem on a Surface

**The Surface.** Let  $\Gamma$  be a smooth, closed, simply connected surface in  $\mathbb{R}^3$  with exterior unit normal  $n$  embedded in a polygonal domain  $\Omega \subset \mathbb{R}^3$ . Let  $U_\delta(\Gamma)$  be the open tubular neighborhood of  $\Gamma$  with thickness  $\delta > 0$ ,

$$U_\delta(\Gamma) = \{x \in \mathbb{R}^3 : |d(x)| < \delta\} \quad (2.1)$$

where  $d(x)$  is the signed distance function of  $\Gamma$  with  $d < 0$  in the interior of  $\Gamma$  and  $d > 0$  in the exterior. Note that  $n = \nabla d$  is the outward-pointing unit normal on  $\Gamma$ . Then there is  $\delta_0 > 0$  such that for each  $x \in U_{\delta_0}(\Gamma)$  the closest point projection:

$$p(x) = x - d(x)n(p(x)) \quad (2.2)$$

maps  $x$  to a unique closest point on  $\Gamma$ . In particular, we require

$$\delta_0 \max_{i=1,2} \|\kappa_i\|_{L^\infty(\Gamma)} < 1 \quad (2.3)$$

where for  $x \in \Gamma$ ,  $\kappa_i$  are the principal curvatures. We also define the extension of a function  $u$  on  $\Gamma$  to  $U_{\delta_0}(\Gamma)$  by

$$u^e(x) = u(p(x)), \quad x \in U_{\delta_0}(\Gamma) \quad (2.4)$$

**The Problem.** We consider the problem: find  $u \in H_0^1(\Gamma) = \{v \in H^1(\Gamma) \mid \int_\Gamma v \, ds = 0\}$  such that

$$a(u, v) = l(v) \quad \forall v \in H_0^1(\Gamma) \quad (2.5)$$

where

$$a(u, v) = \int_{\Gamma} \nabla_{\Gamma} u \cdot \nabla_{\Gamma} v \, ds, \quad l(v) = \int_{\Gamma} f v \, ds \quad (2.6)$$

Here  $\nabla_{\Gamma}$  is the tangential gradient on  $\Gamma$  defined by

$$\nabla_{\Gamma} u = P_{\Gamma} \nabla u^e \quad (2.7)$$

where

$$P_{\Gamma} = I - n \otimes n \quad (2.8)$$

We used the extension of  $u$  which is constant in the normal direction to  $\Gamma$  to formally define  $\nabla_{\Gamma} u$ . However, the tangential derivative depends only on the values of  $u$  on  $\Gamma$  and does not depend on the particular choice of extension.

Using Lax-Milgram's Lemma we conclude that there is a unique solution to (2.5), and we also have the elliptic regularity estimate

$$\|u\|_{H^{s+2}(\Gamma)} \lesssim \|f\|_{H^s(\Gamma)}, \quad s \in \mathbb{Z}, \quad s \geq -1 \quad (2.9)$$

## 3 The Method

### 3.1 The Mesh and Finite Element Space

- *The background mesh and space:* Let  $\mathcal{T}_{h,0}$  be a quasiuniform partition of  $\Omega$  with mesh parameter  $h \in (0, h_0]$  into shape regular tetrahedra. On  $\mathcal{T}_{h,0}$  we define  $V_{h,0}^p$  to be the space of continuous piecewise polynomials of degree  $p \geq 1$ .
- *The discrete surfaces:* Let  $\Gamma_h$  be a sequence of surfaces that converges to  $\Gamma$ . We specify the precise assumptions on the convergence below.
- *The active mesh and the induced surface mesh:* We denote by  $\mathcal{T}_h$  the set consisting of elements in the background mesh  $\mathcal{T}_{h,0}$  that are cut by the discrete geometry  $\Gamma_h$ . These elements form the so called active mesh. See Fig. 1 for an illustration. The restriction of the active mesh to the discrete surface  $\Gamma_h$  manufactures an induced cut surface mesh that we denote by

$$\mathcal{K}_h = \{K = T \cap \Gamma_h : T \in \mathcal{T}_h\} \quad (3.1)$$

- *The finite element space:* The restriction of the background space to the active mesh together with the condition  $\int_{\Gamma_h} v \, ds_h = 0$  defines our finite element space  $V_h^p$ ,

$$V_h^p = \left\{ v_h \in V_{h,0}^p|_{\mathcal{T}_h} : \int_{\Gamma_h} v \, ds_h = 0 \right\} \quad (3.2)$$

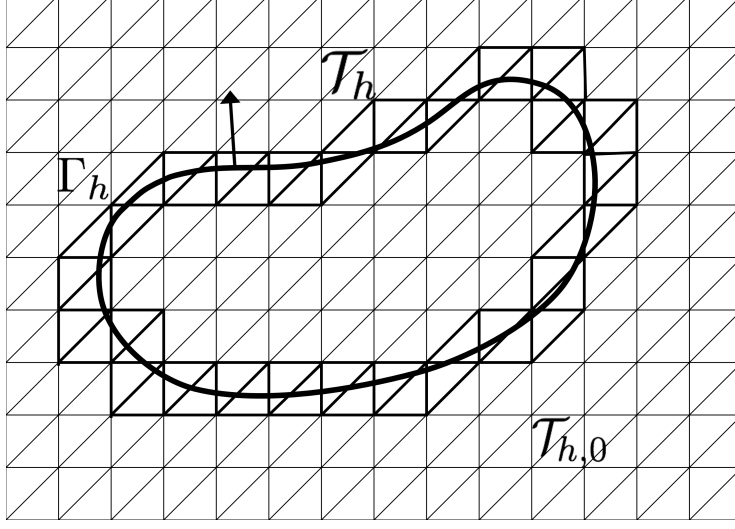


Figure 1: The discrete surface  $\Gamma_h$ , the background mesh  $\mathcal{T}_{h,0}$ , and the active mesh  $\mathcal{T}_h$ .

### 3.2 The Finite Element Method

**Method.** Find  $u_h \in V_h^p$  such that

$$A_h(u_h, v) := a_h(u_h, v) + s_h(u_h, v) = l_h(v) \quad \forall v_h \in V_h^p \quad (3.3)$$

**Forms.**

- The forms  $a_h$  and  $l_h$  are defined by

$$a_h(w, v) = (\nabla_{\Gamma_h} w, \nabla_{\Gamma_h} v)_{\Gamma_h}, \quad l_h(v) = (f_h, v)_{\Gamma_h} \quad (3.4)$$

where the tangential gradient  $\nabla_{\Gamma_h}$  is defined by

$$\nabla_{\Gamma_h} u_h = P_{\Gamma_h} \nabla u_h \quad (3.5)$$

with

$$P_{\Gamma_h} = I - n_h \otimes n_h \quad (3.6)$$

- The stabilization form  $s_h$  is defined by

$$s_h(w, v) = s_{h,F}(w, v) + s_{h,\Gamma}(w, v) \quad (3.7)$$

where

$$s_{h,F}(w, v) = \sum_{j=1}^p c_{F,j} h^{2(j-1+\gamma)} ([D_{n_F}^j w], [D_{n_F}^j v])_{\mathcal{F}_h} \quad (3.8)$$

$$s_{h,\Gamma}(w, v) = \sum_{j=1}^p c_{\Gamma,j} h^{2(j-1+\gamma)} (D_{n_h}^j w, D_{n_h}^j v)_{\mathcal{K}_h} \quad (3.9)$$

Here  $(D_a^j v)|_x$  is the  $j$ :th directional derivative of  $v$  along the line defined by the unit vector  $a(x)$ ,  $[w]_F$  denotes the jump of  $w$  over the face  $F$ ,  $\mathcal{F}_h$  is the set of internal faces (i.e. faces with two neighbors) in the active mesh  $\mathcal{T}_h$ ,  $c_{\Gamma,j} > 0$ ,  $c_{F,j} > 0$  are stabilization parameters, and  $\gamma \in [0, 1]$  is a parameter.

**Remark 3.1** *In the special case  $p = 1$  we obtain*

$$s_h(w, v) = c_F h^{2\gamma} ([D_{n_F}^j w], [D_{n_F}^j v])_{\mathcal{F}_h} + c_\Gamma h^{2\gamma} (D_{n_h}^j w, D_{n_h}^j v)_{\mathcal{K}_h} \quad (3.10)$$

where  $\gamma \in [0, 1]$  which can be compared with the pure face penalty term

$$s_h(w, v) = c_F ([D_{n_F}^j w], [D_{n_F}^j v])_{\mathcal{F}_h} \quad (3.11)$$

developed in [3]. Note that the scalings with the mesh parameter  $h$  are different in the two terms and that for  $\gamma > 0$  the face penalty term is weaker in the stabilization term we introduce here.

### 3.3 Assumptions

**A1.** We assume that the closed, simply connected approximation  $\Gamma_h$  and its unit normal  $n_h$  are such that for all  $h \in (0, h_0]$ ,

$$\|d\|_{L^\infty(\Gamma_h)} \lesssim h^{p+1} \quad (3.12)$$

$$\|n - n_h\|_{L^\infty(\Gamma_h)} \lesssim h^p \quad (3.13)$$

that  $n \cdot n_h > 0$  on  $\Gamma_h$ , and that we have a uniform bound on the curvature  $\kappa_h$ .

**A2.** We assume that the mesh is sufficiently small so that there is a constant  $c$  independent of the mesh size  $h$  such that  $\mathcal{T}_h \subset U_\delta(\Gamma)$  with  $\delta = ch \leq \delta_0$  and that the closest point mapping  $p(x) : \Gamma_h \rightarrow \Gamma$  is a bijection.

**A3.** We assume that the data approximation  $f_h$  is such that  $\| |B| f^e - f_h \|_{L^2(\Gamma_h)} \lesssim h^{p+1} \|f\|_{L^2(\Gamma)}$ . Here  $ds = |B| ds_h$  (see Section 4 for details).

## 4 Preliminary Results

### 4.1 Norms

Given a positive semidefinite bilinear form  $b$  we let  $\|v\|_b^2 = b(v, v)$  denote the associated seminorm. In particular, we will use the following norms on  $V_h^p + H^{p+1}(\mathcal{T}_h)$ ,

$$\|v\|_{a_h}^2 = a_h(v, v), \quad \|v\|_{s_h}^2 = \|v\|_{s_h, F}^2 + \|v\|_{s_h, \Gamma}^2, \quad \|v\|_{A_h}^2 = \|v\|_{a_h}^2 + \|v\|_{s_h}^2 \quad (4.1)$$

We let  $H^s(\omega)$ , with  $\omega \subset \mathbb{R}^d$ , denote the standard Sobolev spaces of order  $s$ . For  $\omega \subset \Gamma$  or  $\omega \subset \Gamma_h$   $H^s(\omega)$  denotes the surface Sobolev space which is based on tangential derivatives.

## 4.2 Some Inequalities

- Under A1 and A2 there is a constant such that the following Poincaré inequality holds for  $h \in (0, h_0]$ ,

$$\|v\|_{L^2(\Gamma_h)} \lesssim \|v\|_{a_h} \quad \forall v \in V_h^p \quad (4.2)$$

see Lemma 4.1 in [3].

- For  $T \in \mathcal{T}_h$  we have the trace inequalities

$$\|v\|_{L^2(\partial T)}^2 \lesssim h^{-1} \|v\|_{L^2(T)}^2 + h \|\nabla v\|_{L^2(T)}^2 \quad v \in H^1(T) \quad (4.3)$$

$$\|v\|_{L^2(T \cap \Gamma_h)}^2 \lesssim h^{-1} \|v\|_{L^2(T)}^2 + h \|\nabla v\|_{L^2(T)}^2 \quad v \in H^1(T) \quad (4.4)$$

where the first inequality is a standard trace inequality, see e.g.[1], and the second inequality is proven in [16] and the constant is independent of how  $\Gamma_h$  intersects  $T$  and of  $h \in (0, h_0]$ .

- For  $T \in \mathcal{T}_h$  we have the inverse inequality

$$\|v\|_{H^j(T)}^2 \lesssim h^{-2(j-s)} \|v\|_{H^s(T)}^2 \quad 0 \leq s \leq j, \quad v \in V_h^p \quad (4.5)$$

see [1].

## 4.3 Interpolation

Let  $\pi_h^p : L^2(\mathcal{T}_h) \rightarrow V_h^p$  be the Scott-Zhang interpolation operator. For all  $v \in H^{p+1}(\mathcal{T}_h)$  and  $T \in \mathcal{T}_h$  the following standard estimate holds

$$\|v - \pi_h^p v\|_{H^m(T)} \lesssim h^{s-m} \|v\|_{H^s(\mathcal{N}_h(T))} \quad m \leq s \leq p+1, \quad m = 0, \dots, p+1 \quad (4.6)$$

where  $\mathcal{N}_h(T) \subset \mathcal{T}_h$  is the union of the elements in  $\mathcal{T}_h$  which share a node with  $T$ . In particular, we have the stability estimate

$$\|\pi_h^p v\|_{H^m(\mathcal{T}_h)} \lesssim \|v\|_{H^m(\mathcal{T}_h)} \quad (4.7)$$

## 4.4 Some Results for Extended and Lifted Functions

**Extension.** Recall that we define the extension of a function  $u$  on  $\Gamma$  to  $U_{\delta_0}(\Gamma)$  by  $u^e(x) = u(p(x))$ . For  $u \in H^s(\Gamma)$ ,  $s \geq 0$  the following holds

$$\|u^e\|_{H^s(U_\delta(\Gamma))} \lesssim \delta^{1/2} \|u\|_{H^s(\Gamma)} \quad (4.8)$$

where  $0 < \delta \leq \delta_0$  and for  $h$  small enough we may take  $\delta \sim h$ . See Lemma 3.1 in [24].

Using the definition of the extension of a function  $u$  on  $\Gamma$ , the definition of the closest point projection (2.2), the chain rule, and the identity  $n = \nabla d$  we obtain

$$\nabla u^e = (P_\Gamma - dH)\nabla u \quad \text{in } U_{\delta_0}(\Gamma) \quad (4.9)$$

where  $H(x) = D^2d(x)$ . For  $x \in U_{\delta_0}(\Gamma)$ , the eigenvalues of  $H(x)$  are  $\kappa_1(x)$ ,  $\kappa_2(x)$ , and 0, with corresponding orthonormal eigenvectors  $a_1(x)$ ,  $a_2(x)$ , and  $n^e(x)$ . We have the identities

$$\kappa_i(x) = \frac{\kappa_i^e(x)}{1 + d(x)\kappa_i^e(x)}, \quad a_i(x) = a_i^e(x), \quad i = 1, 2 \quad (4.10)$$

and  $H(x)$  may be expressed in the form

$$H(x) = \sum_{i=1}^2 \frac{\kappa_i^e(x)}{1 + d(x)\kappa_i^e(x)} a_i^e(x) \otimes a_i^e(x) \quad (4.11)$$

see [13, Lemma 14.7].

Using the fact that  $H$  is tangential,  $P_\Gamma H = H P_\Gamma = H$ , in the identity (4.9) we obtain

$$\nabla u^e = (I - dH)\nabla_\Gamma u \quad (4.12)$$

Thus,

$$\nabla_{\Gamma_h} u^e = B^T \nabla_\Gamma u \quad (4.13)$$

with

$$B = P_\Gamma(I - dH)P_{\Gamma_h} \quad (4.14)$$

**Lifting.** Define the lifting  $v^l$  of a function  $v$  on  $\Gamma_h$  to  $\Gamma$  as

$$(v^l)^e = v^l \circ p = v \quad \text{on } \Gamma_h \quad (4.15)$$

Using equation (4.13) it follows that

$$\nabla_{\Gamma_h} v = \nabla_{\Gamma_h} (v^l)^e = B^T \nabla_\Gamma (v^l) \quad (4.16)$$

and thus we have

$$\nabla_\Gamma (v^l) = B^{-T} \nabla_{\Gamma_h} v \quad (4.17)$$

Here,

$$B^{-1} = \left( I - \frac{n \otimes n_h}{n \cdot n_h} \right) (I - dH)^{-1} \quad (4.18)$$

see [11], and using the fact that  $n$  and  $n_h$  are unit normals it is easy to show that

$$BB^{-1} = P_\Gamma, \quad B^{-1}B = P_{\Gamma_h} \quad (4.19)$$

**Estimates Related to  $B$ .** It can be shown, see [3] for instance, that the following estimates hold

$$\|B\|_{L^\infty(\Gamma_h)} \lesssim 1, \quad \|B^{-1}\|_{L^\infty(\Gamma)} \lesssim 1, \quad \|BB^T - I\|_{L^\infty(\Gamma_h)} \lesssim h^{p+1} \quad (4.20)$$

**Surface Measures.** For the surface measure on  $\Gamma_h$ ,  $ds_h(x)$ , and the surface measure on  $\Gamma$ ,  $ds(p(x))$ , we have the following identity

$$ds(p(x)) = |B(x)|ds_h(x) \quad x \in \Gamma_h \quad (4.21)$$

where

$$|B(x)| = n \cdot n_h(1 - d(x)\kappa_1(x))(1 - d(x)\kappa_2(x)) \quad (4.22)$$

see Proposition A.1 in [11]. Using the identity  $\|n(x) - n_h(x)\|_{\mathbb{R}^3}^2 = 2(1 - n(x) \cdot n_h(x))$  and our assumptions we obtain the following estimates:

$$\|1 - |B|\|_{L^\infty(\Gamma_h)} \lesssim h^{p+1}, \quad \| |B| \|_{L^\infty(\Gamma_h)} \lesssim 1, \quad \| |B|^{-1} \|_{L^\infty(\Gamma_h)} \lesssim 1 \quad (4.23)$$

**Norm Equivalences.** Using the identities (4.13) and (4.17) and the bounds in equations (4.20) and (4.23) we obtain the following equivalences

$$\|v^l\|_{L^2(\Gamma)} \sim \|v\|_{L^2(\Gamma_h)}, \quad \|u\|_{L^2(\Gamma)} \sim \|u^e\|_{L^2(\Gamma_h)} \quad (4.24)$$

and

$$\|\nabla_\Gamma v^l\|_{L^2(\Gamma)} \sim \|\nabla_{\Gamma_h} v\|_{L^2(\Gamma_h)}, \quad \|\nabla_\Gamma u\|_{L^2(\Gamma)} \sim \|\nabla_{\Gamma_h} u^e\|_{L^2(\Gamma_h)} \quad (4.25)$$

We will also use the following bound

$$\|D^j u^e\|_{L^2(\Gamma_h)} \lesssim \|u\|_{H^m(\Gamma)} \quad u \in H^m(\Gamma), \quad j \leq m \quad (4.26)$$

## 5 Properties of the Stabilization Term

Here we formulate properties of a general stabilization term that are sufficient to prove that the resulting linear system of equations have an optimal scaling of the condition number with the mesh parameter compared to standard finite elements and that the convergence of the method is of optimal order.

**Properties.** Let  $s_h$  be a semi positive definite bilinear form such that

**P1.** For  $v \in H^{p+1}(\Gamma) \cap H_0^1(\Gamma)$ ,

$$\|v^e - \pi_h^p v^e\|_{s_h} \lesssim h^p \|v\|_{H^{p+1}(\Gamma)} \quad (5.1)$$

**P2.** For  $v \in H^{p+1}(\Gamma) \cap H_0^1(\Gamma)$ ,

$$\|v^e\|_{s_h} \lesssim h^p \|v\|_{H^{p+1}(\Gamma)} \quad (5.2)$$

**P3.** For  $v \in H^2(\Gamma)$ ,

$$\|\pi_h^p v^e\|_{s_h} \lesssim h \|v\|_{H^2(\Gamma)} \quad (5.3)$$

**P4.** For  $v \in V_h^p$ ,

$$\|v\|_{s_h} \lesssim h^{-3/2} \|v\|_{L^2(\mathcal{T}_h)} \quad (5.4)$$

**P5.** For  $v \in V_h^p$ ,

$$\|v\|_{L^2(\mathcal{T}_h)}^2 \lesssim h(\|v\|_{a_h}^2 + \|v\|_{s_h}^2) \quad (5.5)$$

**Remark 5.1** *The first three properties are used to establish the a priori error estimates: P1 is needed to show optimal interpolation error estimates, P2 is used to estimate the consistency error, and P3 is used to show optimal  $L^2$ -error estimates. In P3 the assumption that  $v \in H^2(\Gamma)$  reflects the fact that the solution to the dual problem resides in  $H^2(\Gamma)$ . The two last properties are used to show the condition number estimate: P4 is the inverse inequality and P5 is the Poincaré inequality. Similar properties have also been stated in [14].*

**Verification of P1–P5.** We now show that the stabilization term defined in (3.7) satisfies P1–P5.

**P1.** Using a standard trace inequality on the faces (4.3) and the trace inequality (4.4) for the contributions on  $\Gamma_h$  we obtain

$$\begin{aligned} \|w\|_{s_h}^2 &= \sum_{j=1}^p \sum_{F \in \mathcal{F}_h} c_{F,j} h^{2(j-1+\gamma)} \| [D_{n_F}^j w] \|_{L^2(F)}^2 \\ &\quad + \sum_{j=1}^p \sum_{K \in \mathcal{K}_h} c_{\Gamma,j} h^{2(j-1+\gamma)} \| D_{n_h}^j w \|_{L^2(K)}^2 \end{aligned} \quad (5.6)$$

$$\lesssim \sum_{j=1}^p \sum_{T \in \mathcal{T}_h} h^{2(j-1+\gamma)} \left( h^{-1} \| D^j w \|_{L^2(T)}^2 + h \| D^{j+1} w \|_{L^2(T)}^2 \right) \quad (5.7)$$

$$\lesssim \sum_{j=0}^p \sum_{T \in \mathcal{T}_h} h^{2(j+\gamma)-1} \| D^{j+1} w \|_{L^2(T)}^2 \quad (5.8)$$

$$= \sum_{j=0}^p h^{2(j+\gamma)-1} \| D^{j+1} w \|_{L^2(\mathcal{T}_h)}^2 \quad (5.9)$$

Next, setting  $w = v^e - \pi_h v^e$ , using the interpolation error estimate (4.6) and the stability (4.8) of the extension operator with  $\delta \sim h$ , we obtain

$$\|v^e - \pi_h v^e\|_{s_h}^2 \lesssim \sum_{j=0}^p h^{2(j+\gamma)-1} \| D^{j+1} (v^e - \pi_h v^e) \|_{L^2(\mathcal{T}_h)}^2 \quad (5.10)$$

$$\lesssim \sum_{j=0}^p h^{2(j+\gamma)-1} h^{2(p-j)} \| D^{j+1} v^e \|_{H^{p+1}(\mathcal{T}_h)}^2 \quad (5.11)$$

$$\lesssim h^{2(p+\gamma)} \|v\|_{H^{p+1}(\Gamma)}^2 \quad (5.12)$$

Finally,  $h^{2(p+\gamma)} \lesssim h^{2p}$  for  $\gamma \in [0, 1]$  since  $h \in (0, h_0]$ , and thus P1 follows.

**P2.** Note first that for  $v \in H^{p+1}(\Gamma)$  we have  $\|v^e\|_{s_h, F} = 0$  and thus  $\|v^e\|_{s_h} = \|v^e\|_{s_h, \Gamma}$ . Next, subtracting  $D_n^j v^e = 0$ , using Assumption A1, and inequality (4.26) we obtain

$$\|v^e\|_{s_h}^2 = \sum_{j=1}^p c_{\Gamma, j} h^{2(j-1+\gamma)} \|D_{n_h}^j v^e\|_{\mathcal{K}_h}^2 \quad (5.13)$$

$$\lesssim \sum_{j=1}^p h^{2(j-1+\gamma)} \|(D_{n_h}^j - D_n^j)v^e\|_{L^2(\mathcal{K}_h)}^2 \quad (5.14)$$

$$\lesssim \sum_{j=1}^p h^{2(j-1+\gamma)} \|n_h - n\|_{L^\infty(\mathcal{K}_h)}^2 \|D^j v^e\|_{L^2(\mathcal{K}_h)}^2 \quad (5.15)$$

$$\lesssim h^{2(p+\gamma)} \|v\|_{H^p(\Gamma)}^2 \quad (5.16)$$

where we used the estimate  $\|n_h - n\|_{L^\infty(\mathcal{K}_h)} \lesssim h^p$ . We conclude that P2 holds for  $\gamma \in [0, 1]$  since  $h \in (0, h_0]$ .

**P3.** For  $w \in V_h^p$  we have the estimate

$$\|w\|_{s_h}^2 \lesssim h^{2\gamma} \|[D_{n_F} w]\|_{L^2(\mathcal{F}_h)}^2 + h^{2\gamma} \|D_{n_h} w\|_{L^2(\mathcal{K}_h)}^2 + h^{2(1+\gamma)-1} \|D^2 w\|_{L^2(\mathcal{T}_h)}^2 \quad (5.17)$$

**Verification of (5.17).** We start from the definition

$$\|w\|_{s_h}^2 = \|w\|_{s_h, F}^2 + \|w\|_{s_h, \Gamma}^2 \quad (5.18)$$

and estimate the two terms on the right hand side as follows. First

$$\|w\|_{s_h, F}^2 \lesssim h^{2\gamma} \|[D_{n_F} w]\|_{L^2(\mathcal{F}_h)}^2 + \sum_{j=2}^p h^{2(j-1+\gamma)} \|[D_{n_F}^j w]\|_{L^2(\mathcal{F}_h)}^2 \quad (5.19)$$

$$\lesssim h^{2\gamma} \|[D_{n_F} w]\|_{L^2(\mathcal{F}_h)}^2 + h^{2(1+\gamma)-1} \|[D^2 w]\|_{L^2(\mathcal{T}_h)}^2 \quad (5.20)$$

where for each  $j = 2, \dots, p$  and each face  $F \in \mathcal{F}_h$  with neighboring elements  $T_1$  and  $T_2$  we used the inverse estimate

$$\|[D_{n_F}^j w]\|_{L^2(F)}^2 \lesssim h^{-1} \|D^j w\|_{L^2(T_1 \cup T_2)}^2 \lesssim h^{-1} h^{2(2-j)} \|D^2 w\|_{L^2(T_1 \cup T_2)}^2 \quad (5.21)$$

Second, using a similar approach

$$\|w\|_{s_h, \Gamma}^2 \lesssim h^{2\gamma} \|D_{n_h} w\|_{L^2(\mathcal{K}_h)}^2 + \sum_{j=2}^p h^{2(j-1+\gamma)} \|D_{n_h}^j w\|_{L^2(\mathcal{K}_h)}^2 \quad (5.22)$$

$$\lesssim h^{2\gamma} \|D_{n_h} w\|_{L^2(\mathcal{K}_h)}^2 + \sum_{j=2}^p \underbrace{h^{2(j-1+\gamma)} h^{-1} h^{2(2-j)}}_{=h^{2(1+\gamma)-1}} \|D^2 w\|_{L^2(\mathcal{T}_h)}^2 \quad (5.23)$$

$$\lesssim h^{2\gamma} \|D_{n_h} w\|_{L^2(\mathcal{K}_h)}^2 + h^{2(1+\gamma)-1} \|D^2 w\|_{L^2(\mathcal{T}_h)}^2 \quad (5.24)$$

where we used the inverse estimate

$$\|D_{n_h}^j w\|_{L^2(K)}^2 \leq \|D^j w\|_{L^2(K)}^2 \lesssim h^{-1} \|D^j w\|_{L^2(T)}^2 \lesssim h^{-1} h^{2(2-j)} \|D^2 w\|_{L^2(T)}^2 \quad (5.25)$$

for  $j = 2, \dots, p$ . Thus (5.17) holds.

Setting  $w = \pi_h v^e$  in (5.17) we obtain

$$\|\pi_h v^e\|_{s_h}^2 \lesssim \underbrace{h^{2\gamma} \| [D_{n_F} \pi_h v^e] \|_{L^2(\mathcal{F}_h)}^2}_I + \underbrace{h^{2\gamma} \| D_{n_h} \pi_h v^e \|_{L^2(\mathcal{K}_h)}^2}_{II} \quad (5.26)$$

$$\begin{aligned} &+ h^{2(1+\gamma)-1} \| D^2 \pi_h v^e \|_{L^2(\mathcal{T}_h)}^2 \\ &= I + II + h^{2(1+\gamma)} \| v \|_{H^2(\Gamma)}^2 \end{aligned} \quad (5.27)$$

where we used the stability of the interpolation operator (4.7) and the stability of the extension operator (4.8). Next we have the following bounds.

**Term I.** Using the fact that  $[D_{n_F} v^e] = 0$  for  $v \in H^2(\Gamma)$  we obtain

$$\| [D_{n_F} \pi_h v^e] \|_{L^2(\mathcal{F}_h)}^2 = \| [D_{n_F} (\pi_h v^e - v^e)] \|_{L^2(\mathcal{F}_h)}^2 \quad (5.28)$$

$$\lesssim h^{-1} \| [D (\pi_h v^e - v^e)] \|_{L^2(\mathcal{T}_h)}^2 + h \| [D^2 (\pi_h v^e - v^e)] \|_{L^2(\mathcal{T}_h)}^2 \quad (5.29)$$

$$\lesssim h \| D^2 v^e \|_{L^2(\mathcal{T}_h)}^2 \quad (5.30)$$

$$\lesssim h^2 \| v \|_{H^2(\Gamma)}^2 \quad (5.31)$$

where we used the trace inequality (4.3), the interpolation estimate (4.6), and finally the stability (4.8) of the extension operator. Thus we have

$$I \lesssim h^{2(1+\gamma)} \| v \|_{H^2(\Gamma)}^2 \quad (5.32)$$

**Term II.** Using the fact that  $D_{n^e} v^e = 0$  we obtain

$$\| D_{n_h} \pi_h v^e \|_{L^2(\mathcal{K}_h)}^2 \lesssim \| D_{n^e} \pi_h v^e \|_{L^2(\mathcal{K}_h)}^2 + \| n^e - n_h \|_{L^\infty(\mathcal{K}_h)}^2 \| D \pi_h v^e \|_{L^2(\mathcal{K}_h)}^2 \quad (5.33)$$

$$\lesssim \| D_n (\pi_h v^e - v^e) \|_{L^2(\mathcal{K}_h)}^2 + h^{2p-1} \| D \pi_h v^e \|_{L^2(\mathcal{T}_h)}^2 \quad (5.34)$$

$$\lesssim h^2 \| v \|_{H^2(\Gamma)}^2 + h^{2p} \| v \|_{H^1(\Gamma)}^2 \quad (5.35)$$

and thus we arrive at

$$II \lesssim h^{2(1+\gamma)} \| v \|_{H^2(\Gamma)}^2 \quad (5.36)$$

since  $p \geq 1$  and  $h \in (0, h_0]$ .

Collecting the bounds we obtain

$$\|\pi_h v^e\|_{s_h} \lesssim h^{1+\gamma} \| v \|_{H^2(\Gamma)} \quad (5.37)$$

and thus P3 holds.

**Simplified Proof of P3 in the Case  $\gamma = 1$ .** Using estimate (5.9) with  $w \in V_h^p$  and inverse inequality (4.5) we obtain

$$\|w\|_{s_h}^2 \lesssim \sum_{j=0}^p h^{2j+1} \|D^{j+1}w\|_{L^2(\mathcal{T}_h)}^2 \quad (5.38)$$

$$\lesssim h \|Dw\|_{L^2(\mathcal{T}_h)}^2 + \underbrace{\sum_{j=1}^p h^{2j+1} \|D^{j+1}w\|_{L^2(\mathcal{T}_h)}^2}_{\lesssim h^3 \|D^2w\|_{L^2(\mathcal{T}_h)}^2} \quad (5.39)$$

$$\lesssim h \|Dw\|_{L^2(\mathcal{T}_h)}^2 + h^3 \|D^2w\|_{L^2(\mathcal{T}_h)}^2 \quad (5.40)$$

Setting  $w = \pi_h v^e$  and using the stability of the interpolation operator (4.7) and the stability of the extension operator (4.8) we obtain

$$\|\pi_h v^e\|_{s_h}^2 \lesssim h \|D\pi_h v^e\|_{L^2(\mathcal{T}_h)}^2 + h^3 \|D^2\pi_h v^e\|_{L^2(\mathcal{T}_h)}^2 \quad (5.41)$$

$$\lesssim h^2 \|v\|_{H^1(\Gamma)}^2 + h^4 \|v\|_{H^2(\Gamma)}^2 \quad (5.42)$$

**P4.** Starting from (5.9) with  $w \in V_h^p$  and using the inverse inequality we get

$$\|w\|_{s_h}^2 \lesssim \sum_{j=0}^p h^{2j+1} \|D^{j+1}w\|_{L^2(\mathcal{T}_h)}^2 \lesssim h^{-1} \|w\|_{L^2(\mathcal{T}_h)}^2 \quad (5.43)$$

Using that  $h \in (0, h_0]$  we have  $h^{-1} \lesssim h^{-3}$  and thus Property P4 holds.

**P5.** See the proof of Lemma 6.3 below.

## 6 Condition Number Estimate

We shall show that the spectral condition number of the stiffness matrix resulting scales as  $h^{-2}$ , independent of the position of the geometry relative to the background mesh. In particular, we show that the stabilization term defined in (3.7) has Property P5 and controls the condition number for linear as well as for higher-order elements.

Let  $\{\varphi_i\}_{i=1}^N$  be a basis in  $V_h^p$  and given  $v \in V_h^p$  let  $\widehat{v} \in \widehat{\mathbb{R}}^N \subset \mathbb{R}^N$  denote the vector containing the coefficients in the expansion:

$$v = \sum_{i=1}^N \widehat{v}_i \varphi_i \quad (6.1)$$

Recall that functions  $v$  in  $V_h^p$  satisfy the condition  $\int_{\Gamma_h} v ds_h = 0$  and therefore  $\widehat{\mathbb{R}}^N$  is

$$\widehat{\mathbb{R}}^N = \{\widehat{v} \in \mathbb{R}^N \mid \widehat{v} \cdot (\int_{\Gamma_h} \varphi_1 ds_h, \dots, \int_{\Gamma_h} \varphi_N ds_h) = 0\} \quad (6.2)$$

Since  $\mathcal{T}_h$  is quasiuniform we have the equivalence

$$\|v\|_{\mathcal{T}_h} \sim h^{d/2} \|\widehat{v}\|_{\widehat{\mathbb{R}}^N} \quad (6.3)$$

where  $d$  is the dimension of the embedding space  $\mathbb{R}^d$ . Let  $\mathcal{A}_h$  be the stiffness matrix associated with  $A_h$ ,

$$(\mathcal{A}_h \widehat{w}, \widehat{v})_{\widehat{\mathbb{R}}^N} = A_h(w, v) \quad \forall v, w \in V_h^p \quad (6.4)$$

and recall that the condition number is defined by

$$\kappa(\mathcal{A}_h) = \|\mathcal{A}_h\|_{\mathbb{R}^N} \|\mathcal{A}_h^{-1}\|_{\mathbb{R}^N} \quad (6.5)$$

which in terms of the eigenvalues of the symmetric positive definite matrix  $\mathcal{A}_h$  is equal to

$$\kappa(\mathcal{A}_h) = \frac{\lambda_N}{\lambda_1} \quad (6.6)$$

where  $\lambda_N$  ( $\lambda_1$ ) is the largest (smallest) eigenvalue of  $\mathcal{A}_h$ .

**Theorem 6.1** *If there are constants, independent of the mesh size  $h$  and of how the surface cuts the background mesh, such that the following hold:*

- *$A_h$  is continuous:*  $A_h(w, v) \lesssim \|w\|_{A_h} \|v\|_{A_h} \quad \forall v, w \in V_h^p + H^{p+1}(\mathcal{T}_h)$
- *$A_h$  is coercive:*  $\|v\|_{A_h}^2 \lesssim A_h(v, v) \quad \forall v \in V_h^p$
- *The inverse inequality:*  $\|v\|_{A_h} \lesssim h^{-3/2} \|v\|_{L^2(\mathcal{T}_h)} \quad v \in V_h^p$
- *The Poincaré inequality:*  $\|v\|_{L^2(\mathcal{T}_h)} \lesssim h^{1/2} \|v\|_{A_h} \quad v \in V_h^p$

Then, the spectral condition number  $\kappa(\mathcal{A}_h)$  satisfies

$$\kappa(\mathcal{A}_h) \lesssim h^{-2} \quad (6.7)$$

**Proof.** For  $v, w \in V_h^p$  it follows from the continuity of the form  $A_h$ , the inverse inequality, and the equivalence between the norms, equation (6.3), that

$$A_h(w, v) \lesssim \|w\|_{A_h} \|v\|_{A_h} \lesssim h^{-3} \|w\|_{L^2(\mathcal{T}_h)} \|v\|_{L^2(\mathcal{T}_h)} \lesssim h^{-3} h^d \|\widehat{w}\|_{\widehat{\mathbb{R}}^N} \|\widehat{v}\|_{\widehat{\mathbb{R}}^N} \quad (6.8)$$

From coercivity, the Poincaré inequality, and the equivalence between the norms, equation (6.3), we obtain

$$A_h(v, v) \gtrsim \|v\|_{A_h}^2 \gtrsim h^{-1} \|v\|_{L^2(\mathcal{T}_h)}^2 \gtrsim h^{-1} h^d \|\widehat{v}\|_{\widehat{\mathbb{R}}^N}^2 \quad (6.9)$$

Using the definition (6.6) of the spectral condition number we get

$$\kappa(\mathcal{A}_h) = \frac{\max_{u \in \widehat{\mathbb{R}}^N, \|\widehat{u}\|_{\widehat{\mathbb{R}}^N} = 1} (\mathcal{A}_h \widehat{u}, \widehat{u})_{\widehat{\mathbb{R}}^N}}{\min_{u \in \widehat{\mathbb{R}}^N, \|\widehat{u}\|_{\widehat{\mathbb{R}}^N} = 1} (\mathcal{A}_h \widehat{u}, \widehat{u})_{\widehat{\mathbb{R}}^N}} \lesssim \frac{h^{-3} h^d}{h^{-1} h^d} = h^{-2} \quad (6.10)$$

□

In the following Lemmas we show that all the conditions in Theorem 6.1 are satisfied.

**Lemma 6.1** (*Continuity and Inf-Sup Condition*) *There is a constant independent of the mesh size  $h$  and of how the surface cuts the background mesh, such that  $A_h$  is continuous:*

$$A_h(w, v) \leq \|w\|_{A_h} \|v\|_{A_h}, \quad \forall v, w \in V_h^p + H^{p+1}(\mathcal{T}_h) \quad (6.11)$$

and  $A_h$  satisfies the inf-sup condition

$$\|w\|_{A_h} \lesssim \sup_{v \in V_h^p \setminus \{0\}} \frac{A_h(w, v)}{\|v\|_{A_h}}, \quad \forall w \in V_h^p \quad (6.12)$$

**Proof.** The continuity follows directly from the Cauchy-Schwarz inequality. The bilinear form  $A_h$  is coercive  $A_h(v, v) = \|v\|_{A_h}^2$  by definition and the inf-sup condition (6.12) follows from coercivity.  $\square$

**Lemma 6.2** (*Inverse Inequality*) *There are constants, independent of the mesh size  $h$  and of how the surface cuts the background mesh, such that the following inverse inequality holds:*

$$\|v\|_{A_h} \lesssim h^{-3/2} \|v\|_{L^2(\mathcal{T}_h)} \quad v \in V_h^p \quad (6.13)$$

**Proof.** Using the element wise trace inequality (4.4), the inverse inequality (4.5), and Property P4 of the stabilization term we obtain

$$\begin{aligned} \|v\|_{a_h}^2 &\lesssim h^{-1} \|v\|_{H^1(\mathcal{T}_h)}^2 + h \|v\|_{H^2(\mathcal{T}_h)}^2 \lesssim h^{-3} \|v\|_{L^2(\mathcal{T}_h)}^2 \\ \|v\|_{s_h}^2 &\lesssim h^{-3} \|v\|_{L^2(\mathcal{T}_h)}^2 \end{aligned} \quad (6.14)$$

Using the above estimates and recalling the definition of  $\|v\|_{A_h}$  the result follows.  $\square$

**Lemma 6.3** (*Poincaré Inequality*) *There are constants, independent of the mesh size  $h$  and of how the surface cuts the background mesh, such that the following Poincaré inequality holds*

$$\|v\|_{L^2(\mathcal{T}_h)} \lesssim h^{1/2} \|v\|_{A_h} \quad v \in V_h^p \quad (6.15)$$

**Proof.** To prove the Poincaré inequality we will proceed in two main steps: 1. We use the face penalty to reach an element which has a large intersection with  $\Gamma_h$ . Here we employ a covering of  $\mathcal{T}_h$ , where each covering set contains elements that have a so called large intersection property, see [3]. 2. For elements with a large intersection the normal derivative control on  $\Gamma_h$  is used to control the  $L^2$  norm on the element.

To establish the Poincaré inequality (6.15) we shall prove that

$$\|v\|_{L^2(\mathcal{T}_h)}^2 \lesssim \sum_{j=0}^p h^{2j+1} \|D_{n_h}^j v\|_{L^2(\Gamma_h)}^2 + \sum_{j=1}^p h^{2j+1} \|[D_{n_F}^j v]\|_{L^2(\mathcal{F}_h)}^2 \quad (6.16)$$

Here we note that (6.15) follows from (6.16) since the right hand side of (6.16) satisfies the estimate

$$\begin{aligned} & \sum_{j=0}^p h^{2j+1} \|D_{n_h}^j v\|_{L^2(\Gamma_h)}^2 + \sum_{j=1}^p h^{2j+1} \|[D_{n_F}^j v]\|_{L^2(\mathcal{F}_h)}^2 \\ & \lesssim h(\|v\|_{\Gamma_h}^2 + h^{2(1-\gamma)}\|v\|_{s_h}^2) \lesssim h(\|v\|_{a_h}^2 + h^{2(1-\gamma)}\|v\|_{s_h}^2) \lesssim h\|v\|_{A_h}^2 \end{aligned} \quad (6.17)$$

where we used the definition (3.7) of  $s_h$ , the Poincaré inequality (4.2), and the fact that  $\gamma \in [0, 1]$ .

**Large Intersection Coverings of  $\mathcal{T}_h$ .** There is a covering  $\{\mathcal{T}_{h,x} : x \in \mathcal{X}_h\}$  of  $\mathcal{T}_h$ , where  $\mathcal{X}_h$  is an index set, such that: (1) Each set  $\mathcal{T}_{h,x}$  contains a uniformly bounded number of elements. (2) Each element in  $\mathcal{T}_{h,x}$  share at least one face with another element in  $\mathcal{T}_{h,x}$ . (3) In each set  $\mathcal{T}_{h,x}$  there is one element  $T_x \in \mathcal{T}_{h,x}$  which has a large intersection with  $\Gamma_h$ ,

$$h^{d-1} \lesssim |T_x \cap \Gamma_h| = |K_x| \quad (6.18)$$

where  $d$  is the dimension. (4) The number of sets  $\mathcal{T}_{h,x}$  to which an element  $T$  belongs is uniformly bounded for all  $T \in \mathcal{T}_h$ . See [3] for the construction of the covering.

We prove (6.16) by considering a set  $\mathcal{T}_{h,x}$  in the covering and the following steps:

**Step 1.** We shall show that

$$\|v\|_{L^2(\mathcal{T}_{h,x})}^2 \lesssim \|v\|_{L^2(T_x)}^2 + \sum_{j=1}^p h^{2j+1} \|[D_{n_F}^j v], [D_{n_F}^j w]\|_{\mathcal{F}_{h,x}} \quad (6.19)$$

where  $\mathcal{F}_{h,x}$  is the set of interior faces in  $\mathcal{T}_{h,x}$ . To prove (6.19) we recall that for two elements  $T_1$  and  $T_2$  that share a face  $F$  it holds

$$\|v\|_{L^2(T_1)}^2 \lesssim \|v\|_{L^2(T_2)}^2 + \sum_{j=1}^p h^{2j+1} \|[D_{n_F}^j v]\|_{L^2(F)}^2 \quad (6.20)$$

see [17] for instance. Now let  $\mathcal{T}_{h,x}^0 = \{T_x\}$  and for  $j = 1, 2, \dots$  let  $\mathcal{T}_{h,x}^j$  be the set of all elements that share a face with an element in  $\mathcal{T}_{h,x}^{j-1}$ . Then there is a uniform constant  $J$  such that  $\mathcal{T}_{h,x}^j = \mathcal{T}_{h,x}^{j-1}$  for  $j \geq J$  and we also have the estimate

$$\|v\|_{\mathcal{T}_{h,x}^j} \lesssim \|v\|_{\mathcal{T}_{h,x}^{j-1}} + \sum_{F \subset \mathcal{F}_{h,x}^j \setminus \mathcal{F}_{h,x}^{j-1}} \sum_{j=1}^p h^{2j+1} \|[D_{n_F}^j v]\|_{L^2(F)}^2 \quad (6.21)$$

where  $\mathcal{F}_{h,x}^j$  is the set of interior faces in  $\mathcal{T}_{h,x}^j$ . Iterating (6.21) we obtain (6.19).

**Step 2.** We shall show that there is a constant such that for all  $T_x \in \mathcal{T}_h$  which have the large intersection property (6.18),

$$\|v\|_{L^2(T_x)}^2 \lesssim \sum_{j=0}^p h^{2j+1} \|D_{n_h}^j v\|_{L^2(K_x)}^2 \quad (6.22)$$

where  $K_x = \Gamma_h \cap T_x$ . To verify (6.22) we define the cylinder

$$\text{Cyl}_\delta(K_x) = \{x \in \mathbb{R}^d : x = y + tn_h, y \in K_x, |t| \leq \delta\} \quad (6.23)$$

and using Taylor's formula for a polynomial  $v \in P_p(\text{Cyl}_\delta(K_x))$ , we obtain the bound

$$\|v\|_{L^2(\text{Cyl}_\delta(K_x))}^2 \lesssim \sum_{j=0}^p \delta^{2j+1} \|D_{n_h}^j v\|_{L^2(K_x)}^2 \quad (6.24)$$

Using the following inverse bound: there is a constant such that for all  $v \in P_p(T_x)$

$$\|v\|_{L^2(T_x)} \lesssim \|v\|_{L^2(\text{Cyl}_\delta(K_x))} \quad (6.25)$$

the desired estimate (6.22) follows for  $\delta \sim h$ .

**Verification of (6.25).** To employ a scaling argument we will construct two regular cylinders with circular cross section and the same center line that may be mapped to a reference configuration, one containing  $T_x$  and one contained in  $\text{Cyl}_\delta(K_x)$ . See Figure 6.

Let  $\bar{F}_x$  be a plane with unit normal  $\bar{n}_x$ , which is tangent to  $K_x$  at an interior point of  $K_x$ . Then we have the bound

$$\|\bar{n}_h - n_h\|_{L^\infty(K_x)} \lesssim h \quad (6.26)$$

and with  $\bar{K}_x$  the closest point projection of  $K_x$  onto  $\bar{F}_x$  we conclude using shape regularity and a uniform bound on the curvature  $\kappa_h$  (Assumption A1) that there is a ball  $\bar{B}_{\bar{r}_1, x} \subset \bar{K}_x \subset \bar{F}_x$  with radius  $\bar{r}_1 \sim h$  and a  $\bar{\delta}_1 \sim h$  such that

$$\text{Cyl}_{\bar{\delta}_1}(\bar{K}_x) = \{x \in \mathbb{R}^d : x = y + t\bar{n}_h, y \in \bar{K}_x, |t| \leq \bar{\delta}_1\} \subset \text{Cyl}_\delta(K_x) \quad (6.27)$$

Next using shape regularity there is a larger ball  $\bar{B}_{\bar{r}_2, x} \subset \bar{F}_x$  with the same center as  $\bar{B}_{\bar{r}_1, x}$  such that

$$\bar{T}_x \subset \bar{B}_{\bar{r}_2, x} \subset \bar{F}_x \quad (6.28)$$

where  $\bar{T}_x$  is the closest point projection of  $T_x$  onto  $\bar{F}_x$ , and a  $\bar{\delta}_2 \sim h$  such that

$$T_x \subset \text{Cyl}_{\bar{\delta}_2}(\bar{B}_{\bar{r}_2, x}) \quad (6.29)$$

Clearly,  $\text{Cyl}_{\bar{\delta}_1}(\bar{B}_{\bar{r}_1, x}) \subset \text{Cyl}_{\bar{\delta}_2}(\bar{B}_{\bar{r}_2, x})$  and using a mapping to a reference configuration we conclude that there is a constant such that for all polynomials  $v \in P_p(\text{Cyl}_{\bar{\delta}_2}(\bar{B}_{\bar{r}_2, x}))$ ,

$$\|v\|_{\text{Cyl}_{\bar{\delta}_2}(\bar{B}_{\bar{r}_2, x})} \lesssim \|v\|_{\text{Cyl}_{\bar{\delta}_1}(\bar{B}_{\bar{r}_1, x})} \quad (6.30)$$

which in view of the inclusions (6.27) and (6.29) concludes the proof of (6.25).

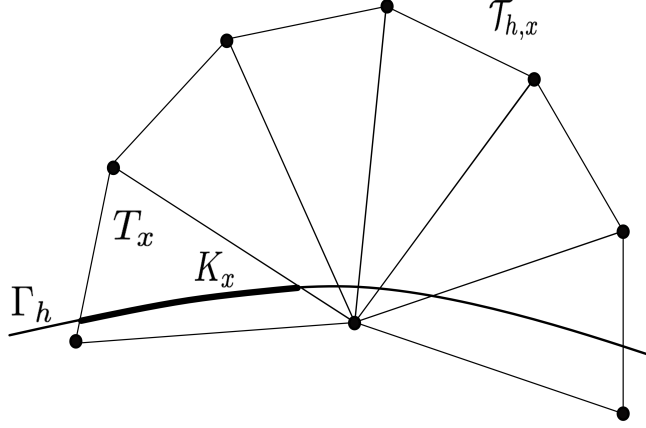


Figure 2: A set of elements  $\mathcal{T}_{h,x}$  in the cover of  $\mathcal{T}_h$ , an element  $T_x$  with large intersection  $K_x = T_x \cap \Gamma_h$ .

**Step 3.** Combining equation (6.19) and (6.22) and using that  $\{\mathcal{T}_{h,x} : x \in \mathcal{X}_h\}$  is a cover of  $\mathcal{T}_h$  completes the proof of (6.16) and the lemma.  $\square$

**Remark 6.1** Using the same technique as in the proof of Lemma 6.3 we may show the stronger estimate

$$\|v\|_{\mathcal{T}_h}^2 + h^{2\gamma} \|\nabla v\|_{\mathcal{T}_h}^2 \lesssim h \|v\|_{A_h}^2 \quad (6.31)$$

where  $\gamma \in [0, 1]$  is the scaling parameter in  $s_h$ , see (3.8) and (3.9). The modifications are as follows. In Step 1 we show that

$$\|\nabla v\|_{L^2(\mathcal{T}_{h,x})}^2 \lesssim \|\nabla v\|_{L^2(T_x)}^2 + \sum_{j=1}^p h^{2j-1} \|[D_{n_F}^j v]\|_{L^2(F)}^2 \quad (6.32)$$

which after multiplication by  $h^{2\gamma}$  corresponds to

$$h^{2\gamma} \|\nabla v\|_{L^2(\mathcal{T}_{h,x})}^2 \lesssim h^{2\gamma} \|\nabla v\|_{L^2(T_x)}^2 + h \left( \sum_{j=1}^p h^{2(j-1+\gamma)} \|[D_{n_F}^j v]\|_{L^2(F)}^2 \right) \quad (6.33)$$

To show (6.32) we use the estimate

$$\|\nabla v\|_{L^2(T_1)}^2 \lesssim \|\nabla v\|_{L^2(T_2)}^2 + \sum_{j=1}^p h^{2j-1} \|[D_{n_F}^j v]\|_{L^2(F)}^2 \quad (6.34)$$

In Step 2 we show that

$$\|\nabla v\|_{L^2(T_x)}^2 \lesssim \|\nabla_{\Gamma_h} v\|_{K_x}^2 + \sum_{j=1}^p h^{2j-1} \|D_{n_h}^j v\|_{L^2(K_x)}^2 \quad (6.35)$$

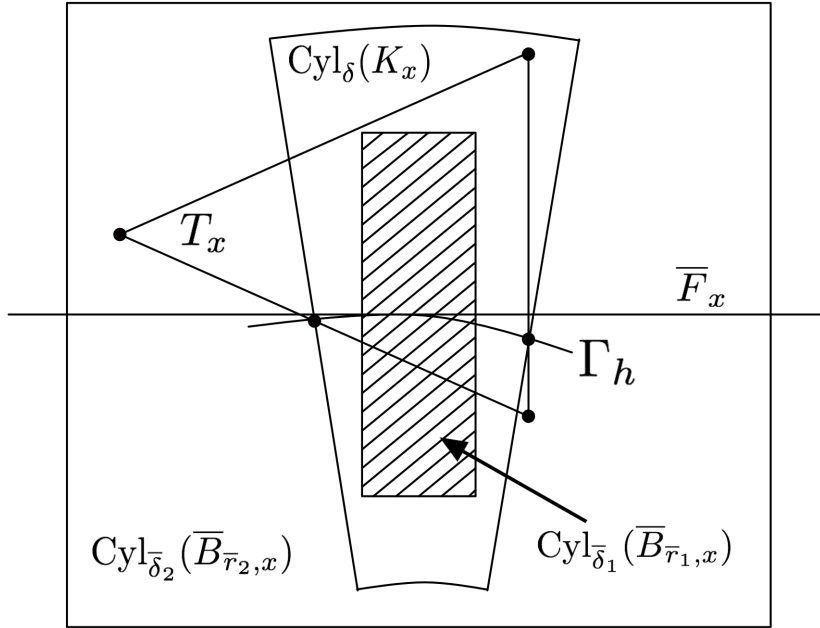


Figure 3: Schematic figure illustrating a typical configuration of an element  $T$ , the curved intersection with  $\Gamma_h$ , the plane  $\bar{F}_x$  which is tangent to  $K_x$ , the cylinders  $\text{Cyl}_\delta(K_x)$ ,  $\text{Cyl}_{\delta_1}(\bar{B}_{\bar{r}_1})$ , and  $\text{Cyl}_{\delta_2}(\bar{B}_{\bar{r}_2})$ . Note that we have the inclusions  $\bar{B}_{\bar{r}_1,x} \subset \bar{K}_x \subset \bar{T}_x \subset \bar{B}_{\bar{r}_2,x}$ ,  $T_x \subset \text{Cyl}_{\delta_2}(\bar{B}_{\bar{r}_2})$ , and  $\text{Cyl}_{\delta_1}(\bar{B}_{\bar{r}_1}) \subset \text{Cyl}_\delta(K_x)$ .

which after multiplication by  $h^{2\gamma}$  corresponds to

$$h^{2\gamma}\|\nabla v\|_{L^2(T_x)}^2 \lesssim \underbrace{h^{2\gamma}\|\nabla_{\Gamma_h} v\|_{K_x}^2}_{\lesssim \|\nabla_{\Gamma_h} v\|_{K_x}^2} + h \left( \sum_{j=1}^p h^{2(j-1+\gamma)} \|D_{n_h}^j v\|_{L^2(K_x)}^2 \right) \quad (6.36)$$

Combining (6.33) and (6.36), summing over the cover, and using Property (4) of the cover we obtain (6.31).

**Remark 6.1** Note the following:

- From (5.43) we see that the scaling of the stabilization term corresponds to the mass matrix. This scaling is the weakest which guarantees the Poincaré inequality (6.15) (Property P4 of the stabilization term).
- For the operator

$$L = \alpha\Delta_{\Gamma} + \beta \quad (6.37)$$

where  $\alpha$  and  $\beta$  are constants, we would have the inverse inequality

$$\|v\|_{A_h} \lesssim (\alpha h^{-3/2} + \beta h^{-1/2}) \|v\|_{\mathcal{T}_h} \quad v \in V_h^P \quad (6.38)$$

instead of (6.13), and the resulting condition number estimate is then

$$\kappa(\mathcal{A}_h) \lesssim \alpha h^{-2} + \beta \quad (6.39)$$

- In the case when

$$\|v\|_{a_h} \lesssim (\alpha h^{-3/2} + \beta h^{-1/2}) \|v\|_{\mathcal{T}_h} \quad (6.40)$$

we note that the desired inverse inequality (6.38) holds for

$$\tilde{s}_h = (\alpha h^{-\tau} + \beta) s_h \quad (6.41)$$

with  $\tau$  in the interval  $0 \leq \tau \leq 2$ , since

$$\|v\|_{\tilde{s}_h}^2 = (\alpha h^{-\tau} + \beta) \|v\|_{s_h}^2 \lesssim (\alpha h^{-\tau} + \beta) h^{-1} \|v\|_{\mathcal{T}_h}^2 \lesssim (\alpha h^{-(1+\tau)} + \beta h^{-1}) \|v\|_{\mathcal{T}_h}^2 \quad (6.42)$$

## 7 A Priori Error Estimates

In this section we prove optimal error estimates in the energy norm and in the  $L^2$  norm.

## 7.1 Strang Lemma

Using that  $A_h$  is continuous and satisfies the inf-sup condition we first show a Strang Lemma which connects the error in the energy norm to the interpolation error and the consistency error.

**Lemma 7.1** *Let  $u \in H_0^1(\Gamma)$  be the unique solution of (2.5) and  $u_h \in V_h^p$  the finite element approximation defined by (3.3). Then the following discretization error bound holds*

$$\|u^e - u_h\|_{A_h} \lesssim \|u^e - \pi_h^p u^e\|_{A_h} + \sup_{v \in V_h^p \setminus \{0\}} \frac{|A_h(u^e, v) - l_h(v)|}{\|v\|_{A_h}} \quad (7.1)$$

**Proof.** Adding and subtracting an interpolant and using the triangle inequality we get

$$\|u^e - u_h\|_{A_h} \leq \|u^e - \pi_h^p u^e\|_{A_h} + \|\pi_h^p u^e - u_h\|_{A_h} \quad (7.2)$$

Using the inf-sup condition (6.12) for  $A_h$  we have

$$\|\pi_h^p u^e - u_h\|_{A_h} \lesssim \sup_{v \in V_h^p \setminus \{0\}} \frac{A_h(\pi_h^p u^e - u_h, v)}{\|v\|_{A_h}} \quad (7.3)$$

Adding and subtracting  $A_h(u^e, v)$  and using the weak formulation (3.3) yields

$$A_h(\pi_h^p u^e - u_h, v) = A_h(\pi_h^p u^e - u^e, v) + A_h(u^e - u_h, v) \quad (7.4)$$

$$= A_h(\pi_h^p u^e - u^e, v) + A_h(u^e, v) - l_h(v) \quad (7.5)$$

Finally, using the continuity of  $A_h$  we obtain

$$A_h(\pi_h^p u^e - u^e, v) \leq \|\pi_h^p u^e - u^e\|_{A_h} \|v\|_{A_h} \quad (7.6)$$

Collecting the estimates we end up with the desired bound

$$\|u^e - u_h\|_{A_h} \lesssim \|u^e - \pi_h^p u^e\|_{A_h} + \sup_{v \in V_h^p \setminus \{0\}} \frac{|A_h(u^e, v) - l_h(v)|}{\|v\|_{A_h}} \quad (7.7)$$

□

## 7.2 The Interpolation Error

Next we prove optimal interpolation error estimates using Property P1 of the stabilization term.

**Lemma 7.2** *For all  $u \in H^{p+1}(\Gamma)$  we have the following estimate*

$$\|u^e - \pi_h^p u^e\|_{A_h} \lesssim h^p \|u\|_{H^{p+1}(\Gamma)} \quad (7.8)$$

**Proof.** From the definition of the energy norm  $\|\cdot\|_{A_h}$ , equation (4.1), we have

$$\|u^e - \pi_h^p u^e\|_{A_h}^2 = \underbrace{\|u^e - \pi_h^p u^e\|_{a_h}^2}_I + \underbrace{\|u^e - \pi_h^p u^e\|_{s_h}^2}_{II} \quad (7.9)$$

**Term I.** Using the element wise trace inequality (4.4), standard interpolation estimates (4.6) on elements  $T \in \mathcal{T}_h$ , and the stability estimate (4.8) for the extension operator with  $\delta \sim h$ , we obtain

$$I = \|u^e - \pi_h^p u^e\|_{a_h}^2 \quad (7.10)$$

$$\lesssim \sum_{T \in \mathcal{T}_h} \left( h^{-1} \|u^e - \pi_h^p u^e\|_{H^1(T)}^2 + h \|u^e - \pi_h^p u^e\|_{H^2(T)}^2 \right) \quad (7.11)$$

$$\lesssim h^{2p-1} \|u^e\|_{H^{p+1}(\mathcal{T}_h)}^2 \quad (7.12)$$

$$\lesssim h^{2p} \|u\|_{H^{p+1}(\Gamma)}^2 \quad (7.13)$$

**Term II.** From Property P1 of the stabilization term we have that

$$II \lesssim h^{2p} \|u\|_{H^{p+1}(\Gamma)}^2 \quad (7.14)$$

Combining the two estimates (7.10) and (7.14) the result follows.  $\square$

### 7.3 The Consistency Error

The approximation of the geometry  $\Gamma$  by  $\Gamma_h$  and the approximation of the data  $f$  by  $f_h$  leads to a consistency error that we estimate in the next lemma.

**Lemma 7.3** *Let  $u \in H^{p+1}(\Gamma) \cap H_0^1(\Gamma)$  be the solution of (2.5) then, the following bound holds*

$$\sup_{v \in V_h^p \setminus \{0\}} \frac{|A_h(u^e, v) - l_h(v)|}{\|v\|_{A_h}} \lesssim h^p \|u\|_{H^{p+1}(\Gamma)} + h^{p+1} \|f\|_{L^2(\Gamma)} \quad (7.15)$$

**Proof.** We have the identity

$$|A_h(u^e, v) - l_h(v)| \leq \underbrace{|a_h(u^e, v) - l_h(v)|}_I + \underbrace{|s_h(u^e, v)|}_{II} \quad (7.16)$$

**Term I.** Adding  $-a(u, v^l) + l(v^l) = 0$ , and using the triangle inequality

$$I \leq \underbrace{|a_h(u^e, v) - a(u, v^l)|}_{I_I} + \underbrace{|l(v^l) - l_h(v)|}_{I_{II}} \quad (7.17)$$

**Term  $I_I$ .** Adding and subtracting  $\int_{\Gamma_h} \nabla_{\Gamma_h} u^e \cdot \nabla_{\Gamma_h} v |B| ds_h$ , using that  $B^T B^{-T} = P_{\Gamma_h}$ , changing the domain of integration from  $\Gamma$  to  $\Gamma_h$ , using the triangle inequality, norm

equivalences in (4.25), estimates (4.20), and (4.23) we obtain

$$\begin{aligned}
|a_h(u^e, v) - a(u, v^l)| &= \left| \int_{\Gamma_h} (1 - |B|) \nabla_{\Gamma_h} u^e \cdot \nabla_{\Gamma_h} v \, ds_h \right. \\
&\quad + \int_{\Gamma_h} B^T (B^{-T} \nabla_{\Gamma_h} u^e) \cdot B^T (B^{-T} \nabla_{\Gamma_h} v) |B| \, ds_h \\
&\quad \left. - \int_{\Gamma_h} (B^{-T} \nabla_{\Gamma_h} u^e) \cdot (B^{-T} \nabla_{\Gamma_h} v) |B| \, ds_h \right| \\
&\lesssim \left( \|1 - |B|\|_{L^\infty(\Gamma_h)} + \|BB^T - I\|_{L^\infty(\Gamma_h)} \right) \|\nabla_{\Gamma} u\|_{L^2(\Gamma)} \|\nabla_{\Gamma_h} v\|_{L^2(\Gamma_h)} \\
&\lesssim h^{p+1} \|\nabla_{\Gamma} u\|_{L^2(\Gamma)} \|v\|_{a_h}
\end{aligned} \tag{7.18}$$

**Term  $I_{II}$ .** Changing the domain of integration we get

$$|l(v^l) - l_h(v)| = \left| \int_{\Gamma} f v^l \, ds - \int_{\Gamma_h} f_h v \, ds_h \right| \tag{7.19}$$

$$= \left| \int_{\Gamma_h} f^e v |B| \, ds_h - \int_{\Gamma_h} f_h v \, ds_h \right| \tag{7.20}$$

$$\lesssim \| |B| f^e - f_h \|_{L^2(\Gamma_h)} \|v\|_{L^2(\Gamma_h)} \tag{7.21}$$

$$\lesssim h^{p+1} \|f\|_{L^2(\Gamma)} \|v\|_{L^2(\Gamma)} \tag{7.22}$$

where we at last used Assumption A3 on the data approximation  $f_h$ . Together, the bounds of  $I_I$  and  $I_{II}$ , and the Poincaré inequality (4.2), imply

$$I \lesssim h^{p+1} \|\nabla_{\Gamma} u\|_{L^2(\Gamma)} \|v\|_{a_h} + h^{p+1} \|f\|_{L^2(\Gamma)} \|v\|_{L^2(\Gamma_h)} \tag{7.23}$$

$$\lesssim (\|\nabla_{\Gamma} u\|_{L^2(\Gamma)} + \|f\|_{L^2(\Gamma)}) h^{p+1} \|v\|_{a_h} \tag{7.24}$$

Finally, using that  $u$  is the solution of (2.5) we have the stability estimate  $\|\nabla_{\Gamma} u\|_{L^2(\Gamma)} \lesssim \|f\|_{L^2(\Gamma)}$ , and we obtain

$$I \lesssim h^{p+1} \|f\|_{L^2(\Gamma)} \|v\|_{a_h} \tag{7.25}$$

**Term  $II$ .** Using the Cauchy-Schwarz inequality and Property P2 of the stabilization term, see Section 5, we obtain

$$|s_h(u^e, v)| \lesssim \|u^e\|_{s_h} \|v\|_{s_h} \lesssim h^p \|u\|_{H^{p+1}(\Gamma)} \|v\|_{s_h} \tag{7.26}$$

Combining the estimates of  $I$  and  $II$  we obtain the desired estimate

$$|A_h(u^e, v) - l_h(v)| \lesssim h^p \|u\|_{H^{p+1}(\Gamma)} \|v\|_{A_h} + h^{p+1} \|f\|_{L^2(\Gamma)} \|v\|_{a_h} \tag{7.27}$$

□

## 7.4 Error Estimates

We first prove optimal error estimates in the energy norm and then apply a duality argument to obtain  $L^2$ -error estimates

**Theorem 7.1** *Let  $u \in H^{p+1}(\Gamma) \cap H_0^1(\Gamma)$  be the solution of (2.5) and  $u_h \in V_h^p$  the finite element approximation defined by (3.3). If assumptions A1-A3 hold and the stabilization term has properties P1-P5 then, there is a constant independent of the mesh size  $h$  such that the following error bound holds*

$$\|u^e - u_h\|_{A_h} \lesssim h^p \|u\|_{H^{p+1}(\Gamma)} + h^{p+1} \|f\|_{L^2(\Gamma)} \quad (7.28)$$

**Proof.** Using the Strang Lemma followed by the bounds on the interpolation error (7.8) and the consistency error (7.15) we get the desired bound.  $\square$

**Theorem 7.2** *Let  $u \in H^{p+1}(\Gamma) \cap H_0^1(\Gamma)$  be the solution of (2.5) and  $u_h \in V_h^p$  the finite element approximation defined by (3.3). If assumptions A1-A3 hold and the stabilization term has properties P1-P5 then, there is a constant independent of the mesh size  $h$  such that the following error bound holds*

$$\|u^e - u_h\|_{L^2(\Gamma_h)} \lesssim h^{p+1} \|u\|_{H^{p+1}(\Gamma)} + h^{p+1} \|f\|_{L^2(\Gamma)} \quad (7.29)$$

**Proof.** The proof is similiar to the proof of the  $L^2$ -error estimate in [3] for  $p = 1$ . Let  $e_h = u^e - u_h|_{\Gamma_h}$  and its lift on  $\Gamma$  be  $e_h^l = u - u_h^l$ . Recall that  $\int_{\Gamma} u \, ds = 0$  and  $\int_{\Gamma_h} u_h \, ds_h = 0$ . We now define  $\tilde{u}_h \in V_h^p$  as

$$\tilde{u}_h = u_h - |\Gamma|^{-1} \int_{\Gamma} u_h^l \, ds \quad (7.30)$$

so that we have  $\int_{\Gamma} \tilde{u}_h^l = 0$ . By adding and subtracting  $\tilde{u}_h^l$  and using the triangle inequality we obtain

$$\|e_h^l\|_{L^2(\Gamma)} \leq \underbrace{\|u - \tilde{u}_h^l\|_{L^2(\Gamma)}}_I + \underbrace{\|\tilde{u}_h^l - u_h^l\|_{L^2(\Gamma)}}_{II} \quad (7.31)$$

**Term I.** Consider the dual problem:

$$a(v, \phi) = (\psi, v)_{\Gamma}, \quad \psi \in L^2(\Gamma) \setminus \mathbb{R} \quad (7.32)$$

It follows from the Lax-Milgram lemma that there exists a unique solution in  $H^1(\Gamma) \setminus \mathbb{R}$  and we also have the elliptic regularity estimate

$$\|\phi\|_{H^2(\Gamma)} \lesssim \|\psi\|_{L^2(\Gamma)} \quad (7.33)$$

Setting  $v = u - \tilde{u}_h^l$  in (7.32), adding and subtracting an interpolant, and using the weak formulations in (2.5) and (3.3) we obtain

$$(u - \tilde{u}_h^l, \psi)_\Gamma = a(u - \tilde{u}_h^l, \phi) \quad (7.34)$$

$$= a(u - \tilde{u}_h^l, \phi - (\pi_h^p \phi^e)^l) + a(u - \tilde{u}_h^l, (\pi_h^p \phi^e)^l) \quad (7.35)$$

$$= \underbrace{a(u - \tilde{u}_h^l, \phi - (\pi_h^p \phi^e)^l)}_{I_I} + \underbrace{l((\pi_h^p \phi^e)^l) - l_h(\pi_h^p \phi^e)}_{I_{II}} \quad (7.36)$$

$$+ \underbrace{a_h(\tilde{u}_h, \pi_h^p \phi^e) - a(\tilde{u}_h^l, (\pi_h^p \phi^e)^l)}_{I_{III}} + \underbrace{s_h(\tilde{u}_h, \pi_h^p \phi^e)}_{I_{IV}} \quad (7.37)$$

**Term  $I_I$ .** Using the Cauchy-Schwarz inequality, the norm equivalences (see Section 4), and the energy norm estimate (Theorem 7.1) we obtain

$$I_I \lesssim \|\nabla_\Gamma(u - \tilde{u}_h^l)\|_{L^2(\Gamma)} \|\nabla_\Gamma(\phi - (\pi_h^p \phi^e)^l)\|_{L^2(\Gamma)} \quad (7.38)$$

$$\lesssim \|u^e - u_h\|_{a_h} \|\phi^e - \pi_h^p \phi^e\|_{a_h} \quad (7.39)$$

$$\lesssim (h^p \|u\|_{H^{p+1}(\Gamma)} + h^{p+1} \|f\|_{L^2(\Gamma)}) \|\phi^e - \pi_h^p \phi^e\|_{a_h} \quad (7.40)$$

The interpolation error estimate (7.10) with  $s = 1$  yields

$$\|\phi^e - \pi_h^p \phi^e\|_{a_h} \lesssim h \|\phi\|_{H^2(\Gamma)} \quad (7.41)$$

and finally using the elliptic regularity estimate (7.33) we get

$$I_I \lesssim (h^{p+1} \|u\|_{H^{p+1}(\Gamma)} + h^{p+2} \|f\|_{L^2(\Gamma)}) \|\psi\|_{L^2(\Gamma)} \quad (7.42)$$

**Term  $I_{II} - I_{III}$ .** We use the estimate of Term  $I$  in the proof of Lemma 7.3, together with the following stability estimate

$$\|\nabla_\Gamma \tilde{u}_h^l\|_{L^2(\Gamma)} = \|\nabla_\Gamma u_h^l\|_{L^2(\Gamma)} \lesssim \|u_h\|_{a_h} \lesssim \|f_h\|_{L^2(\Gamma_h)} \lesssim \|f\|_{L^2(\Gamma)} \quad (7.43)$$

to get

$$|I_{II} + I_{III}| \lesssim (h^{p+1} \|\nabla_\Gamma \tilde{u}_h^l\|_{L^2(\Gamma)} + h^{p+1} \|f\|_{L^2(\Gamma)}) \|\pi_h^p \phi^e\|_{a_h} \lesssim h^{p+1} \|f\|_{L^2(\Gamma)} \|\pi_h^p \phi^e\|_{a_h} \quad (7.44)$$

Adding and subtracting an interpolant, using the interpolation error estimate (7.41) followed by the elliptic regularity estimate (7.33) yield

$$\|\pi_h^p \phi^e\|_{a_h} \lesssim \|\pi_h^p \phi^e - \phi^e\|_{a_h} + \|\phi^e\|_{a_h} \lesssim \|\phi\|_{H^2(\Gamma)} \lesssim \|\psi\|_{L^2(\Gamma)} \quad (7.45)$$

Thus,

$$|I_{II} + I_{III}| \lesssim h^{p+1} \|f\|_{L^2(\Gamma)} \|\psi\|_{L^2(\Gamma)} \quad (7.46)$$

**Term  $I_{IV}$ .** We have

$$|I_{IV}| = |s_h(u_h, \pi_h^p \phi^e)| \lesssim \|u_h\|_{s_h} \|\pi_h^p \phi^e\|_{s_h} \quad (7.47)$$

Using the energy norm error estimate, Theorem 7.1, and Property P2 of the stabilization we obtain

$$\|u_h\|_{s_h} \lesssim \|u_h - u^e\|_{s_h} + \|u^e\|_{s_h} \quad (7.48)$$

$$\lesssim h^p \|u\|_{H^{p+1}(\Gamma)} + h^{p+1} \|f\|_{L^2(\Gamma)} + h^p \|u\|_{H^{p+1}(\Gamma)} \quad (7.49)$$

and using Property P3 and the elliptic regularity estimate (7.33) we obtain

$$\|\pi_h^p \phi^e\|_{s_h} \lesssim h \|\phi\|_{H^2(\Gamma)} \lesssim h \|\psi\|_{L^2(\Gamma)} \quad (7.50)$$

We thus have

$$|I_{IV}| \lesssim (h^{p+1} \|u\|_{H^{p+1}(\Gamma_h)} + h^{p+2} \|f\|_{L^2(\Gamma)}) \|\psi\|_{L^2(\Gamma)} \quad (7.51)$$

**Final Estimate of Term  $I$ .** Collecting the estimates of Terms  $I_I - I_{IV}$  and taking  $\psi = u - \tilde{u}_h^l / \|u - \tilde{u}_h^l\|_{L^2(\Gamma)}$  we obtain

$$I = \|u - \tilde{u}_h^l\|_{L^2(\Gamma)} \lesssim h^{p+1} \|u\|_{H^{p+1}(\Gamma_h)} + h^{p+1} \|f\|_{L^2(\Gamma)} \quad (7.52)$$

**Term  $II$ .** Using the definition (7.30) of  $\tilde{u}_h$ , adding  $\int_{\Gamma_h} u_h ds_h = 0$ , changing the domain of integration and using related bounds, employing the Poincaré inequality (4.2), and the stability estimate (7.43), we obtain

$$\|\tilde{u}_h^l - u_h^l\|_{L^2(\Gamma)} = \left| \int_{\Gamma} u_h^l ds - \int_{\Gamma_h} u_h ds_h \right| \quad (7.53)$$

$$\lesssim \left| \int_{\Gamma_h} u_h (|B| - 1) ds_h \right| \quad (7.54)$$

$$\lesssim h^{p+1} \|u_h\|_{L^2(\Gamma_h)} \quad (7.55)$$

$$\lesssim h^{p+1} \|u_h\|_{a_h} \quad (7.56)$$

$$\lesssim h^{p+1} \|f\|_{L^2(\Gamma)} \quad (7.57)$$

**Conclusion of the Proof.** Using the estimates of Terms  $I$  and  $II$  in equation (7.31) and the equivalence  $\|e_h^l\|_{L^2(\Gamma)} \sim \|e_h\|_{L^2(\Gamma_h)}$  conclude the proof.  $\square$

## 8 Numerical Examples

Let the interface  $\Gamma$  be a circle of radius 1 centered at the origin. We generate a uniform triangular mesh with  $h = h_{x_1} = h_{x_2}$  on the computational domain:  $[-1.5, 1.5] \times [-1.5, 1.5]$  where the interface is embedded.

**Conditioning and Convergence Study For the Laplace-Beltrami Problem.** A right-hand side  $f$  to equation (2.5) is calculated so that

$$u(x, t) = e^{-4t}x_1x_2 + x_1^3x_2^2 \quad (8.1)$$

is the exact solution. We discretize (2.5) using the proposed CutFEM with polynomials of degree  $p=1, 2$ , and  $3$ . We choose the stabilization constants in (3.7)-(3.9) to be  $c_{F,j} = c_{\Gamma,j} = \frac{10^{-1}}{j!}$ ,  $j = 1, \dots, p$  and  $\gamma = 1$ .

In Fig. 4 we show the error and the condition number of the linear systems as a function of the mesh size  $h$ . The error measured in the  $L^2$  norm behaves as  $\mathcal{O}(h^{p+1})$  and in the  $H^1$  norm as  $\mathcal{O}(h^p)$ , as expected. The condition number behaves as  $\mathcal{O}(h^{-2})$  independent of the polynomial degree and how the interface cuts the background mesh. However, the constant in the  $\mathcal{O}(h^{-2})$  estimate increases as the polynomial degree increases. We always show the condition number using the  $L^1$  norm which is an estimate of the spectral condition number.

The stabilization term developed in [3] can be written in the form (3.7)-(3.9) with  $c_{\Gamma,j} = 0$  for all  $j$  and  $\gamma = 0$ . Therefore, we refer to it as the pure face stabilization. We choose  $c_{F,j} = \frac{10^{-1}}{j!}$ ,  $j = 1, \dots, p$ . In Fig. 5 and 6 we show the effect of the stabilization on the error and the condition number using linear ( $p=1$ ) and cubic elements ( $p=3$ ). We show the convergence only with respect to the  $L^2$  norm since the results are similar when the error is measured in the  $H^1$  norm. The proposed stabilization, represented by circles, is compared to using no stabilization, i.e.,  $c_{F,j} = c_{\Gamma,j} = 0$ , represented by diamonds, and the pure face stabilization, represented by stars. For linear elements the  $L^2$  norm of the errors using the different stabilizations and no stabilization are very similar but we clearly see that when no stabilization is used the condition number can become extremely large depending on the position of the interface relative the background mesh. For higher order elements the linear systems are severely ill-conditioned without stabilization and therefore the behaviour of the error is oscillatory and depends on how the geometry cuts the background mesh. When the approximation of the interface is slightly changed the magnitude of the error and the convergence shown in Fig. 6, may change a lot for the unstabilized method. Using the pure face stabilization we see that the  $L^2$  norm of the error initially decrease as the mesh size decreases but when the condition number becomes to large the convergence stops and rounding errors start to dominate. Note that the condition numbers are very large also for course meshes. With the proposed stabilization we obtain both optimal convergence orders and the condition number scales as  $\mathcal{O}(h^{-2})$  independent of how the interface cuts the background mesh. Decreasing the constant in the stabilization decreases the magnitude of the error but the condition number increases. Our choice of constants in the stabilization term are not optimized and other choices may give better results.

**Conditioning Study for the Mass Matrix.** We now consider the problem of finding  $u_h \in V_h^p$  such that

$$\int_{\Gamma_h} u_h v_h ds_h + s_h(u_h, v_h) = \int_{\Gamma_h} f_h v_h ds_h \quad (8.2)$$

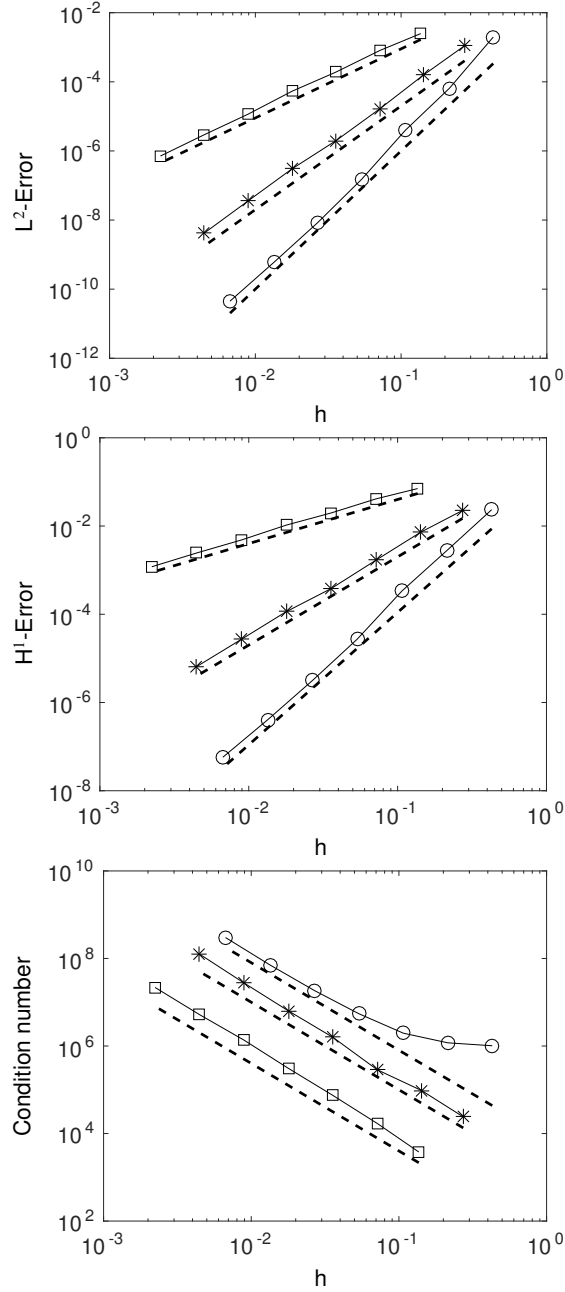


Figure 4: The Laplace-Beltrami equation: The error and condition number versus mesh size  $h$  for different degrees of polynomials,  $p$ , in the discretization. Squares:  $p=1$ . Stars:  $p=2$ . Circles:  $p=3$ . The stabilization constants are  $c_{F,j} = c_{r,j} = \frac{10^{-1}}{j!}$ ,  $j = 1, \dots, p$ . Top: The error measured in the  $L^2$  norm versus mesh size  $h$ . The dashed lines are indicating the expected rate of convergence and are proportional to  $h^{p+1}$ . Middle: The error measured in the  $H^1$  norm versus mesh size  $h$ . The dashed lines are indicating the expected rate of convergence and are proportional to  $h^p$ . Bottom: The condition number versus mesh size  $h$ . The dashed lines are all proportional to  $h^{-2}$ .

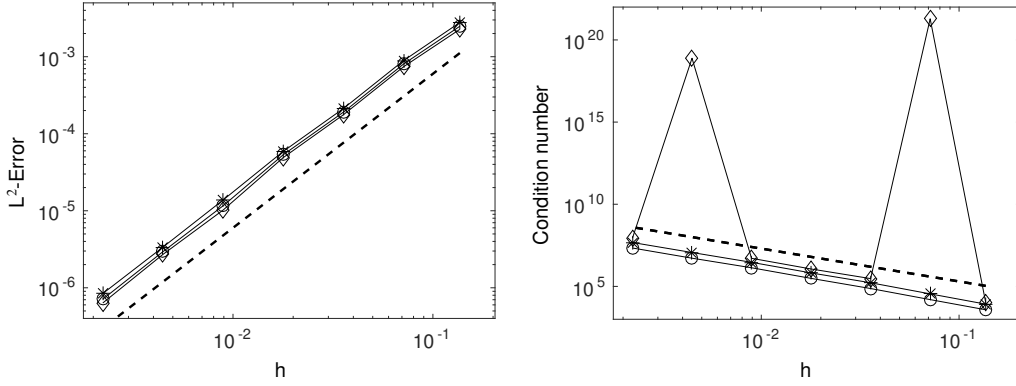


Figure 5: The Laplace-Beltrami equation: The error and condition number versus mesh size  $h$  using different stabilization parameters. Linear elements are used, i.e.  $p=1$ . Circles: the proposed stabilization. Stars: the pure face stabilization developed in [3]. Diamonds: no stabilization is added. Left: The error measured in the  $L^2$  norm versus mesh size  $h$ . The dashed line is indicating the expected rate of convergence and is proportional to  $h^2$ . Right: The condition number versus mesh size  $h$ . The dashed line is proportional to  $h^{-2}$ .

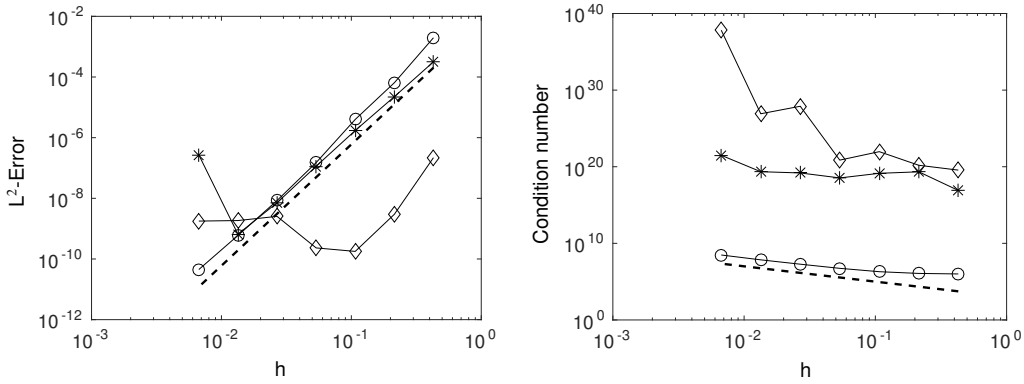


Figure 6: The Laplace-Beltrami equation: The error and condition number versus mesh size  $h$  using different stabilization parameters. Cubic elements are used, i.e.  $p=3$ . Circles: the proposed stabilization. Stars: the pure face stabilization. Diamonds: no stabilization is added. Left: The error measured in the  $L^2$  norm versus mesh size  $h$ . The dashed line is indicating the expected rate of convergence and is proportional to  $h^4$ . Right: The condition number versus mesh size  $h$ . The dashed line is proportional to  $h^{-2}$ .

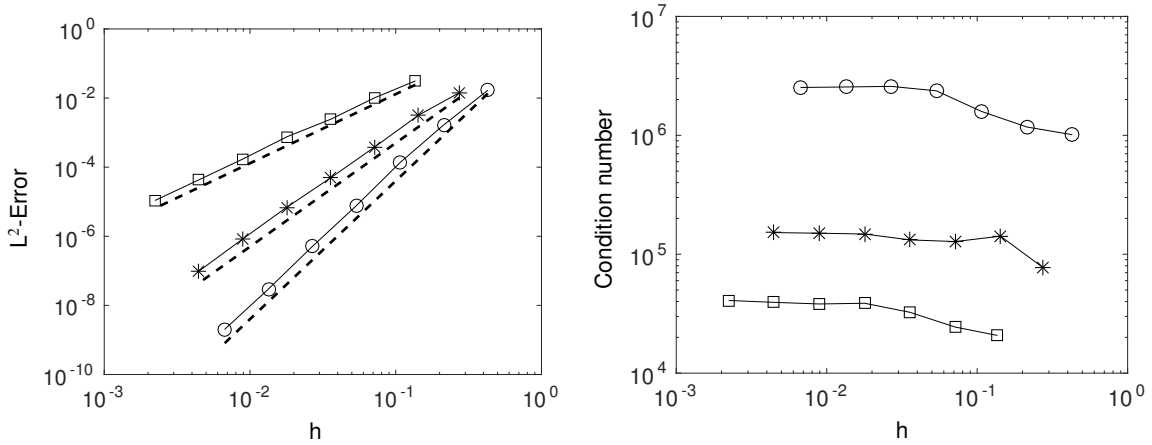


Figure 7: The mass matrix: The error and condition number versus mesh size  $h$  for different degrees of polynomials,  $p$ , in the space discretization. Squares:  $p=1$ . Stars:  $p=2$ . Circles:  $p=3$ . Left: The error measured in the  $L^2$  norm versus mesh size  $h$ . The dashed lines are indicating the expected rate of convergence and are proportional to  $h^{p+1}$ . Right: The condition number versus mesh size  $h$ .

where  $s_h$  is the stabilization term defined in (3.7). We let  $f_h$  be:

$$f_h = \frac{-(2x^5 - 17x^3y^2 + 6xy^4)}{x^2 + y^2} \quad (8.3)$$

We study the condition number of the mass matrix using different degrees of polynomials,  $p$ , and different stabilization terms. Fig. 7 shows that the stabilization term we propose results in optimal convergence rates in the  $L^2$  norm and optimal scaling of the condition number ( $\mathcal{O}(1)$ ) of the mass matrix as it did for the Laplace-Beltrami operator. The constant in the condition number estimate however depends on the polynomial degree. We have chosen  $c_{F,j} = c_{\Gamma,j} = \frac{10^{-4}}{j!}$ ,  $j = 1, \dots, p$  and  $\gamma = 1$ . Increasing these constants decreases the condition number but the magnitude of the error increases. Our choice of constants in the stabilization term are not optimized and other choices could give better results.

In Fig. 8 and 9 we compare different stabilization terms for linear and cubic elements, respectively. We use the proposed stabilization with  $c_{F,j} = c_{\Gamma,j} = \frac{10^{-4}}{j!}$ ,  $j = 1, \dots, p$ , the pure face stabilization, i.e.  $c_{\Gamma,j} = 0$  for all  $j$ ,  $c_{F,j} = \frac{10^{-4}}{j!}$ ,  $j = 1, \dots, p$ , the pure interface stabilization i.e.  $c_{F,j} = 0$  for all  $j$ ,  $c_{\Gamma,j} = \frac{10^{-4}}{j!}$ ,  $j = 1, \dots, p$ , with  $\gamma = 1$  in all cases. Our observations are similar to what we observed for the Laplace-Beltrami operator. For higher order elements the linear systems are severely ill-conditioned without stabilization and the behaviour of the error is oscillatory and the convergence rate will depend on how the geometry cuts the background mesh. We also see that neither the pure face stabilization nor a pure interface stabilization give enough control of the condition number and that we need, as we propose, the combination of them.

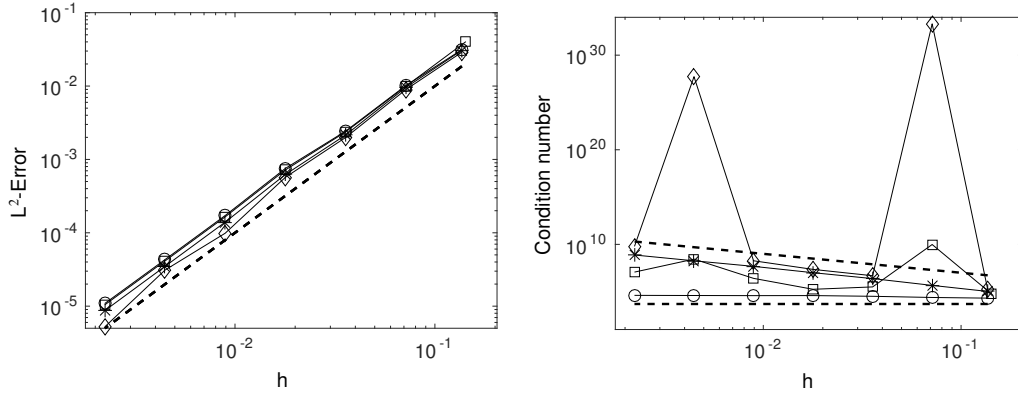


Figure 8: The mass matrix: The error and condition number versus mesh size  $h$  using different stabilization parameters. Linear elements are used, i.e.  $p=1$ . Circles: the proposed stabilization. Stars: the pure face stabilization. Diamonds: no stabilization is added. Left: The error measured in the  $L^2$  norm versus mesh size  $h$ . The dashed line is indicating the expected rate of convergence and is proportional to  $h^2$ . Right: The condition number versus mesh size  $h$ . The dashed lines are proportional to  $h^{-2}$  and  $h^0$ .

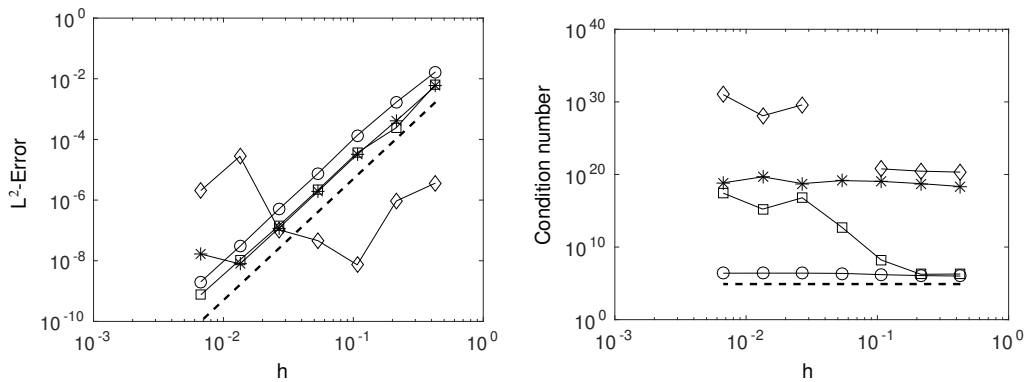


Figure 9: The mass matrix: The error and condition number versus mesh size  $h$  using different stabilization parameters. Cubic elements are used, i.e.  $p=3$ . Circles: the proposed stabilization. Stars: pure face stabilization. Diamonds: no stabilization is added. Squares: pure interface stabilization. Left: The error measured in the  $L^2$  norm versus mesh size  $h$ . The dashed line is indicating the expected rate of convergence and is proportional to  $h^4$ . Right: The condition number versus mesh size  $h$ . The dashed line is proportional to  $h^0$ .

## References

- [1] S. C. Brenner and L. R. Scott. *The Mathematical Theory of Finite Element Methods*. Springer-Verlag, 2008.
- [2] E. Burman, S. Claus, P. Hansbo, M. G. Larson, and A. Massing. CutFEM: discretizing geometry and partial differential equations. *Internat. J. Numer. Methods Engrg.*, 104(7):472–501, 2015.
- [3] E. Burman, P. Hansbo, and M. G. Larson. A stabilized cut finite element method for partial differential equations on surfaces: the Laplace-Beltrami operator. *Comput. Methods Appl. Mech. Engrg.*, 285:188–207, 2015.
- [4] E. Burman, P. Hansbo, M. G. Larson, and A. Massing. Cut finite element methods for partial differential equations on embedded manifolds of arbitrary codimensions. *ArXiv e-prints*, October 2016.
- [5] E. Burman, P. Hansbo, M. G. Larson, and A. Massing. A cut discontinuous Galerkin method for the Laplace-Beltrami operator. *IMA J. Numer. Anal.*, 37(1):138–169, 2017.
- [6] E. Burman, P. Hansbo, M. G. Larson, A. Massing, and S. Zahedi. Full gradient stabilized cut finite element methods for surface partial differential equations. *Comput. Methods Appl. Mech. Engrg.*, 310:278–296, 2016.
- [7] E. Burman, P. Hansbo, M. G. Larson, and S. Zahedi. Cut finite element methods for coupled bulk-surface problems. *Numer. Math.*, 133(2):203–231, 2016.
- [8] M. Cenanovic, P. Hansbo, and M. G. Larson. Minimal surface computation using a finite element method on an embedded surface. *Internat. J. Numer. Methods Engrg.*, 104(7):502–512, 2015.
- [9] M. Cenanovic, P. Hansbo, and M. G. Larson. Cut finite element modeling of linear membranes. *Comput. Methods Appl. Mech. Engrg.*, 310:98–111, 2016.
- [10] K. Deckelnick, C. M. Elliott, and T. Ranner. Unfitted finite element methods using bulk meshes for surface partial differential equations. *SIAM J. Numer. Anal.*, 52(4):2137–2162, 2014.
- [11] A. Demlow and G. Dziuk. An adaptive finite element method for the Laplace-Beltrami operator on implicitly defined surfaces. *SIAM J. Numer. Anal.*, 45(1):421–442 (electronic), 2007.
- [12] A. Demlow and M. A. Olshanskii. An adaptive surface finite element method based on volume meshes. *SIAM J. Numer. Anal.*, 50(3):1624–1647, 2012.

- [13] D. Gilbarg and N. S. Trudinger. *Elliptic partial differential equations of second order*. Classics in Mathematics. Springer-Verlag, Berlin, 2001. Reprint of the 1998 edition.
- [14] J. Grande, C. Lehrenfeld, and A. Reusken. Analysis of a high order trace finite element method for pdes on level set surfaces. *ArXiv e-prints*, November 2016.
- [15] S. Gross, M. A. Olshanskii, and A. Reusken. A trace finite element method for a class of coupled bulk-interface transport problems. *ESAIM Math. Model. Numer. Anal.*, 49(5):1303–1330, 2015.
- [16] A. Hansbo, P. Hansbo, and M. G. Larson. A finite element method on composite grids based on Nitsche’s method. *M2AN Math. Model. Numer. Anal.*, 37(3):495–514, 2003.
- [17] P. Hansbo, M. G. Larson, and K. Larsson. Cut finite element methods for linear elasticity problems. *ArXiv e-prints*, March 2017.
- [18] P. Hansbo, M. G. Larson, and S. Zahedi. A cut finite element method for coupled bulk-surface problems on time-dependent domains. *Comput. Methods Appl. Mech. Engrg.*, 307:96–116, 2016.
- [19] M. A. Olshanskii and A. Reusken. A finite element method for surface PDEs: matrix properties. *Numer. Math.*, 114(3):491–520, 2010.
- [20] M. A. Olshanskii and A. Reusken. Error analysis of a space-time finite element method for solving PDEs on evolving surfaces. *SIAM J. Numer. Anal.*, 52(4):2092–2120, 2014.
- [21] M. A. Olshanskii, A. Reusken, and J. Grande. A finite element method for elliptic equations on surfaces. *SIAM J. Numer. Anal.*, 47(5):3339–3358, 2009.
- [22] M. A. Olshanskii, A. Reusken, and X. Xu. An Eulerian space-time finite element method for diffusion problems on evolving surfaces. *SIAM J. Numer. Anal.*, 52(3):1354–1377, 2014.
- [23] M. A. Olshanskii, A. Reusken, and X. Xu. A stabilized finite element method for advection-diffusion equations on surfaces. *IMA J. Numer. Anal.*, 34(2):732–758, 2014.
- [24] A. Reusken. Analysis of trace finite element methods for surface partial differential equations. *IMA J. Numer. Anal.*, 35(4):1568–1590, 2015.
- [25] S. Zahedi. A space-time cut finite element method with quadrature in time. In *Geometrically Unfitted Finite Element Methods and Applications - Proceedings of the UCL Workshop 2016*, Lecture Notes in Computational Science and Engineering. Springer.